Long-term functional recovery and associated microbial community structure after sediment drying and bedform migration

Anna Oprei[1]*, José Schreckinger[1], Tatiana Kholiavko[2], Aline Frossard[3], Michael Mutz[1] and Ute Risse-Buhl[4,5,6]

[1]Department of Aquatic Ecology, Brandenburg University of Technology Cottbus-Senftenberg, Bad Saarow, Germany, [2]Department of Soil Protection and Recultivation, Brandenburg University of Technology Cottbus-Senftenberg, Cottbus, Germany, [3]Forest Soil and Biogeochemistry, Swiss Federal Research Institute WSL, Birmensdorf, Switzerland, [4]Department of River Ecology, Helmholtz Centre for Environmental Research—UFZ, Magdeburg, Germany, [5]Institute for Environmental Sciences, RPTU Kaiserslautern-Landau, Landau, Germany, [6]Ecology Department, Faculty of Biology, RPTU Kaiserslautern-Landau, Kaiserslautern, Germany

Climate change and erosion from agricultural areas cause increased drying periods and bedform migration of riverbeds, respectively, worldwide. Both sediment drying and bedform migration can independently stress the microbial community residing in the riverbed. Here, we investigated the microbial response after exposure to these stressors with a focus on long-term recovery. We conducted an *in situ* experiment to investigate the long-term (8 months) functional and structural recovery of benthic microbial communities from either sediment drying (episodic severe stressor) or bedform migration (frequent moderate stressor). Stressed sediment associated communities were rewetted (dried sediments) and immobilized (migrated sediments) and exposed in the River Spree (north-eastern Germany) to initiate the recovery process. We then evaluated the microbial function (community respiration, net community production and extracellular enzymatic activities) as well as the bacterial, fungal and diatom community structure (16S rRNA gene and ITS region metabarcoding, and microscopic diatom morphotype classification). We observed different recovery times for community respiration (less than 7 days) and gross primary production (more than 5 months), implying a shift toward net heterotrophy in the first few months after stress exposure. Similarly, we observed a strong autotrophic community response (particularly associated with the diatoms *Navicula* and *Fragilaria*), especially in migrated sediments. The bacterial and fungal community response to sediment drying was stronger than to bedform migration (particularly associated with the bacterium *Flavobacterium* and the fungi *Alternaria* sp. and *Aureobasidium pullulans*). Our results show that sediment drying and bedform migration had a significant impact on the microbial community function and structure, which persisted for several months after the stress. Due to the surprising long period of recovery, successive stress events combined with seasonal effects will likely hamper the ongoing recovery process with severe alterations to the microbial function and structure. These findings extend the concept of ecosystem resilience and stability on the dimensions of timescale and seasonal environmental variations. Legacy effects are expected to play a key role when facing future stress.

Introduction

Lotic ecosystems have been recognized as important drivers of the global carbon cycle (Cole et al., 2007; Aufdenkampe et al., 2011; Raymond et al., 2013) and maintenance of regional biodiversity (Naiman et al., 1993; Dudgeon et al., 2006; Meyer et al., 2007). However, the integrity and functioning of important biogeochemical processes and ecosystem services are regularly challenged by the exposure to stressors (Elosegi et al., 2010; Smeti et al., 2019). A stressor, either natural or anthropogenic, is any factor that alters steady-state environmental conditions (abiotic or biotic) and influences the growth or mortality of organisms in a community (Rocca et al., 2019). Microbial communities colonizing the riverbed have gained wide acceptance as sensitive indicators of environmental change in recent years (Burns and Ryder, 2001; Feio et al., 2010; Lau et al., 2015) as they contribute substantially to the biogeochemical cycling of organic matter and nutrients (Besemer, 2015; Battin et al., 2016; Leff et al., 2016). Hence, impacts of stress on lotic ecosystems are often paralleled by changes in microbial community structure and benthic metabolism, which are both viable features for ecosystem functioning (Battin et al., 2003; Bell et al., 2005). In the case where the microbial community structure is heavily altered by a stress, metabolism may still be unaffected due to functional redundancy, which describes that different species perform similar ecological functions and, therefore, ensure stable ecosystem functioning despite species loss (Lawton and Brown, 1993; Loreau, 2004; Wohl et al., 2004). The response of a microbial community to stress can be described by resistance and resilience, two important drivers of community stability (Allison and Martiny, 2008; Shade et al., 2012; Rocca et al., 2019; Pelletier et al., 2020). Resistance is the ability to withstand functional and structural changes during stress exposure (Pimm, 1984; Allison and Martiny, 2008). Resilience is the capacity to return to the original state of activity and community structure when the exposure to stress has ended (Holling, 1973). Community recovery describes the return of a system to either its pre-disturbance state or a comparable control (Power, 1998; Shade et al., 2012; Sorensen and Shade, 2020).

Some of the most harmful stresses for benthic microbial communities are the absence of water as well as increased radiation and temperature during drought periods. Sediment drying becomes increasingly frequent in temperate perennial streams as a consequence of climate change (Vörösmarty et al., 2000; Döll and Schmied, 2012; Wanders and Van Lanen, 2015). Microbial communities of perennial streams show a reduced resistance toward water scarcity compared to those of temporary streams (Timoner et al., 2020). Ample evidence manifests the high potential of drying periods to alter biogeochemical cycling (Vázquez et al., 2015; Sabater et al., 2016; Colls et al., 2019), microbial community composition and abundance (Febria et al., 2012; Fazi et al., 2013; Gionchetta et al., 2020), trophic interactions (Ledger et al., 2013; Oprei et al., 2019) and gas fluxes to the atmosphere (Gómez-Gener et al., 2016; Muñoz et al., 2018; Bolpagni et al., 2019). Flow resumption after drought entails the activation of dormant

microbes and the leaching of carbon and nutrients that accumulated during the preceding drying phase (Larned et al., 2010; Romaní et al., 2017; von Schiller et al., 2017), fuelling microbial activity during the first biogeochemical response.

Another common phenomenon in temperate streams is the accumulation of sandy sediments that dominate the riverbed of lowland rivers. Rivers draining agricultural areas are vulnerable to increased input of sandy sediments as a result of catchment erosion (Matthaei et al., 2006; Belmont et al., 2011; Wilkes et al., 2019). These sandy riverbeds are mobile and form migrating bedforms, such as sand ripples, at flow velocities of <0.2 to $0.6\,m\,s^{-1}$ (Langlois and Valance, 2007; Charru et al., 2013). Bedform migration alters the hyporheic exchange of solutes and fines (Packman and Brooks, 2001; Harvey et al., 2012; Zheng et al., 2019) and impacts oxygen fluxes in and underneath the bedform (Rutherford et al., 1993; Ahmerkamp et al., 2015; Wolke et al., 2020). Migrating bedforms negatively affect community respiration (Zlatanović et al., 2017; Scheidweiler et al., 2021) and primary production (Uehlinger et al., 2002; Marcarelli et al., 2015; Scheidweiler et al., 2021) in comparison to sediments that are immobile (stationary), providing reasons to see bedform migration as a moderate stress.

The impacts of stress on aquatic ecosystems, for example, severe drought, have been noted to persist long after conditions have returned to normal (Rees et al., 2006; Calapez et al., 2014; Truchy et al., 2020). However, many experimental studies evaluated only short-term responses after drying in the scale of days (McKew et al., 2011; Oprei et al., 2019) to weeks (Pohlon et al., 2013; Gionchetta et al., 2019; Truchy et al., 2020) and after bedform migration in the scale of days (Scheidweiler et al., 2021), ignoring potential lagged stress effects at longer temporal scales.

Microbiological processes range in the scale of several hours to a few days (Song et al., 2014; Wieder et al., 2015) and are quickly restored at the community level due to functional redundancy (Comte et al., 2013; Woodward et al., 2015; Louca et al., 2018), while structural responses lag behind (Berga et al., 2012). Since the response to stress is not monotonous, and includes decoupling of functional and structural recovery, extrapolating short-term responses is likely to be erroneous (Berga et al., 2012; König et al., 2017). This further highlights the necessity of monitoring the recovery on a long-term scale (Niemi et al., 1990; Berga et al., 2012). Despite numerous studies on multiple stressor effects in aquatic ecosystems (e.g., Nõges et al., 2016; Romero et al., 2018; Cabrerizo et al., 2019), direct comparisons between the recovery paths from different stresses under comparable environmental conditions are scarce. It is known that the recovery path of the microbial community is shaped by the previous stress type (König et al., 2017) as well as its strength and frequency (Berga et al., 2012).

Studies on soil suggest that microbial communities with a history of stress have the ability to adapt their response to future stress and increase their resistance and resilience (Evans and Wallenstein, 2012; van Kruistum et al., 2018). Unlike in Mediterranean streams where riverbed biofilms experience a history of periodic drying through seasonal droughts, drying in most temperate rivers is episodic and a

rather rare stress despite ongoing hydrological shifts under climate change. On the contrary, bedform migration in sandy lowland streams can be addressed as a frequent stress, since shifting between stationary patches of sands and migrating bedforms is caused regularly by fluctuations in discharge and bed patch dynamics (migration history; Zlatanović et al., 2017; Scheidweiler et al., 2021).

Our field experiment in a sand bed river aimed to assess the functional and structural recovery of benthic microbial communities that had been exposed to one of two types of stress: (i) drying or (ii) bedform migration. In lowland steams, these stressors can occur at distinct points in time, but sometimes also in spatial and temporal proximity. The recovery paths of the sediment microbial communities were investigated for 8 months after they were rewetted and deposited at rest on the riverbed. We intended to cover the transition of short- to mid-term (days to 1–2 weeks) to long-term recovery (weeks to months). Microbial communities from permanently wet and stationary riverbed sediments served as a control. We hypothesized that (1) microbial communities recover functionally and structurally from previous stresses in the long term irrespective of the stressor type. Furthermore, based on the assumption of functional redundancy, (2) functional recovery is faster than structural recovery, independent of the stressor type. Linked to the role of stress intensity on the recovery, we further expected that (3) communities that have been exposed to drying (episodic and severe stress) show slower functional and structural recovery compared to communities that have been exposed to bedform migration (periodic and moderate stress).

Materials and methods

Study site

The experiment was performed in the third order sand bed lowland River Spree approximately 10 km north of Cottbus (north-eastern Germany, UTM coordinates 51°50′N and 14°20′E). The area is characterized by a temperate continental climate with a yearly precipitation of 568 mm [DWD Climate Data Center (CDC), 2020]. Riparian vegetation is dominated by scattered willow (*Salix* spp.) and alder (*Alnus glutinosa*) trees. The experimental reach is approximately 100 m long. Discharge has a long-term (1979–2020) annual mean of $15.4 \, m^3 s^{-1}$ and varies between 8.2 $m^3 s^{-1}$ (mean low flow) and $39.8 \, m^3 s^{-1}$ (mean high flow) at the nearest gauge in Cottbus (see Supplementary Figure S1 for a hydrograph between January 2018– June 2019). The River Spree is categorized as rarely intermittent (*sensu* Datry et al., 2017). An extraordinarily severe and long drought period in autumn and winter 2018 had decreased the discharge to <5 $m^3 s^{-1}$, exposing large parts of the riverbed to drying. The riverbed is composed of grain sizes in the range of sand (D_{50}: 0.65 mm, D_{10}: 0.30 mm, D_{85}: 1.6 mm). At base flow, more than half of the riverbed in the study reach was covered by migrating ripples. The migration velocity of these bedforms ranged at 6–69 cm h^{-1} with a median of 38.6 cm h^{-1} at mean low flow.

Experimental design

We performed a field experiment by comparing the function and structure of benthic microbial communities that recovered from either drying (hereafter dried) or bedform migration (hereafter migrated) to a control, which was submerged and immobile (hereafter control). To prepare the dried sediment, we sampled fully submerged and immobile (hereafter stationary) sandy sediment from the top 10 cm of the riverbed in June 2018 (Supplementary Figures S2A,B). The sediment was dried for 90 days under an outdoor translucent rooftop, exposed to natural sunlight radiation and temperature changes without shading and excluding precipitation (for details of the drying process see Schreckinger et al., 2021). Migrated and control sediments were sampled from the crest (≤1 cm) of migrating bedform and stationary sediment patches, respectively, at base flow in October 2018 (Supplementary Figure S2C). All three sediment types (dried, migrated, control) were sieved (<2 mm) before approximately 200 mL of each sediment type were transferred into 20 × 26 cm mesh bags (250 μm mesh size; Supplementary Figure S2D). The mesh bags (four replicates per sediment type) were fixed to a rope with roughly 20 cm distance between adjacent bags (Supplementary Figure S2E). This was repeated seven times for the subsequent sampling times (seven ropes with 12 mesh bags each from three sediment types) and all mesh bags were placed on the riverbed by fixing the ropes with steel pegs (Supplementary Figure S2F).

The field experiment started when we exposed the mesh bags in the river, rewetting the dried sediment and immobilizing the formerly migrating sediments. We started the recovery of dried and migrated sediments in late autumn (22 October 2018) as drying naturally occurs during the summer months, therefore, inevitably designating autumn/winter as the primary starting point for microbial recovery. One set of sediment samples was not immersed in the river but analyzed on the same day and served as initial characterization (day 0). The sediment exposed to the river was further retrieved after 4, 7, 21, 42, 105, 161, and 224 days (Supplementary Figure S2G). At each sampling date, we additionally sampled submerged, stationary sediment (i.e., not in mesh bags) next to the exposed bags to account for possible mesh bag effects and seasonal dynamics (hereafter *in situ*). All samples were stored cool and dark during the transport to the laboratory (<2 h). Subsamples for community respiration (CR) and net community production (NCP) were analyzed immediately. Subsamples for potential extracellular enzyme activities (EEA), bacterial and fungal community structure analyses, and autotrophic biomass (Chlorophyll a: Chl a) were stored at −20°C until further processing. Subsamples for characterizing the autotrophic (cyanobacteria and eukaryotic algae) community structure were fixed with Lugol (10% final concentration).

Environmental parameters

The water temperature in the river was monitored continuously with HOBO data loggers (HOBO Pendant® Temperature/Light 64 K Data Logger and HOBO Water Temperature Pro v2 Data Logger, Onset Computer Corporation, Massachusetts, United States). Daily discharge was retrieved from the gauge in Cottbus (Landesamt für Umwelt Brandenburg). Dissolved organic carbon (DOC) was measured from three replicates of filtered river water (0.45 μm, Sartorius) using high-temperature combustion (DIMATOC 2000, Dimatec Analysentechnik GmbH, Essen, Germany). Nitrate (NO_3-N), nitrite (NO_2-N), ammonium (NH_4-N) and soluble reactive phosphorous (SRP) were photometrically determined in triplicate

(0.2 μm filtered river water, Sartorius) using the segmented flow analyzer (DIN EN ISO 13395-D28, 1996; DIN EN ISO 11732-E23, 2005; DIN EN ISO 15681 Part 2-D46, 2005; respectively). All samples were stored at 4°C in the dark until analyzing them 1 day after sampling.

Community respiration and net community production

At each sampling day, about 18 mL of sediment (46 g DW) were transferred from each mesh bag into microcosms (30 mL glass syringes, FORTUNA OPTIMA, Poulten & Graf GmbH, Wertheim, Germany). The microcosms were filled with filtered (250 μm) oxygen-saturated river water and sealed with an airtight silicone plug without head space. They were placed into a water bath for temperature control at 11°C. Peristaltic pumps (ISMATEC ISM932D, Cole-Parmer GmbH, Wertheim, Germany) perfused each microcosm from bottom to top with filtered river water (mean ± standard deviation of all sampling dates: DOC: 4.21 ± 0.27 mg C L^{-1}, DIN: 1.83 ± 0.66 mg N L^{-1}, SRP: 10.48 ± 7.02 μg P L^{-1}) at 0.5 ml min^{-1} (24–27 min perfusion time). The microcosms were exposed to dark (14 ± 2 h) and light periods [10 ± 3 h, LED strips (SolarStringer SunStrip, daylight, Econlux, Cologne, Germany)] for 72 h, mirroring the current season-dependent duration of daylight in the field. Dissolved oxygen (DO) in the water was measured through valves at the inlet and outlet of the perfusing water of each microcosm with a needle-type oxygen microsensor (NTH-PSt1, Precision Sensing GmbH, Regensburg, Germany; accuracy: $\pm 0.4\%$ at 20.2% O$_2$). The latter had been calibrated with a two-point calibration (oxygen-free and oxygen-saturated water) before use. The difference in DO before and after sediment perfusion was taken as a proxy for CR in dark and for NCP in light. The gross primary production (GPP) was obtained by subtracting CR from every NCP measurement (individually for each microcosm), according to the light and dark bottle method (Gaarder and Gran, 1927). CR and GPP rates (μg O$_2$ h^{-1} g DW^{-1}) were related to the dry weight (DW) of the sediment and residence time of the sediment pore water in the microcosm, and standardized to 20°C using the temperature normalization by Winkler et al. (1996) with a Q$_{10}$ factor of 2.

Potential extracellular enzyme activities

Potential EEA were assayed for β-glucosidase (BG), β-xylosidase (BX), alkaline phosphatase (AP), chitinase (NAG), leucine aminopeptidase (LAP), phenol oxidase (PO), and phenol peroxidase (PP), in order to capture the major metabolic pathways in aerobic sediments that include carbon, nitrogen and phosphorous (Frossard et al., 2012). Each of the enzyme activities was measured at three specific sampling dates (0, 21, and 105 days of recovery) and three replicates per sediment type were prepared by adding 2 g DW of sediment to 60 ml of buffer solution (0.1 M trishydroxyaminomethane, pH 7–9) in an autoclaved glass beaker. The slurry solution was agitated with a magnetic stirrer for 30 s. Four technical replicates of each sample slurry (200 μL) were pipetted into a black (for BG, BX, AP, NAG, and LAP assays) or transparent microplate well (for PO and PP assays). Subsequently, 50 μL of substrate analog solution (200 μM) was added. We used 4-methylumbelliferone (MUB; for the BG, BX, NAG

and AP assays) and 7-amino-4-methylcoumarin (AMC; for the LAP assay) as fluorescent molecules linked to substrates, and dihydroxyphenylalanine (L-DOPA) for the PO and PP assays. An amount of 10 μL of 0.3% H$_2$O$_2$ was added to the well of the PP assays.

We filled extra wells with sample slurry without substrate for sample control and substrate without sample slurry to correct for variations in fluorescence and absorbance. Quenching was assessed and corrected for by calculating the ratio of fluorescence of each sample spiked with a fluorescent standard (MUB or AMC) and the respective standard with a buffer solution. The following incubation period (1.5 h) was conducted at 11°C, under constant darkness and mild stirring. An amount of 10 μL NaOH 0.5 N was added at the end of the incubation to terminate the reaction. The fluorescence and absorbance were measured with an Infinite 200 fluorometer (Tecan, Männedorf, Switzerland) at excitation/emission wavelengths of 365/445 nm for BG, BX, AP and NAG, 365/450 nm for LAP, and 365/460 nm for PO and PP, respectively. The potential EEA were calculated as μmol h^{-1} mL^{-1} and also standardized to 20°C (Q$_{10}$ factor of 2; Winkler et al., 1996). We used CR, GPP and EEA measurements to reflect the microbial community function as suggested by a sound body of literature (e.g., Cardinale et al., 2002; Young and Collier, 2009; Freimann et al., 2013; Gionchetta et al., 2019; Baattrup-Pedersen et al., 2020).

Bacterial and fungal community analysis

Bacterial and fungal community structure was assessed by amplicon sequencing on three replicates per treatment at 0, 21, and 105 days of recovery. The DNA was extracted from about 0.5 g DW of each sediment sample with DNeasy Powersoil kits (Qiagen, Hilden, Germany) and quantified with the PicoGreen dsDNA quantification kit (Thermo Fisher, Waltham, MA, United States). We targeted and amplified the 16S rRNA$_{V3-V4}$ genomic region (Bacteria) using primer pairs 341Fh/806R and the ITS2 region (Fungi) using primer pairs ITS3/ITS4 (Perez-Mon et al., 2020). The reaction mix for the polymerase chain reaction (PCR) was created by mixing 10 ng of DNA extract with GoTaq® Flexi Buffer 5x (5 μL), MgCl$_2$ 25 mM (2.5 μL), forward and reverse primer 100 μM (each 0.2 μL), dNTP 10 mM (0.5 μL), BSA 30 mg mL^{-1} (0.5 μL), Hot start Taq 5 U μL^{-1} (0.25 μL) and ddH$_2$0 (8.4 μL). The PCR was initiated for 2 min at 95°C, followed by 36 (Bacteria) or 38 (Fungi) amplification cycles, and concluded with a final elongation stage for 10 min at 72°C. Each amplification cycle included denaturation of the extract for 40 s at 94°C, annealing of the primer for 40 s at 58°C, and elongation for 1 min at 72°C. The PCRs were run three times and pooled afterwards. Amplicons were sent to the Génome Québec Innovation Center at McGill University (Montréal, Canada) where they were purified, quantified, barcoded and paired-end sequenced using the Illumina MiSeq v3 platform (Illumina Inc., San Diego, Ca, United States).

A customized pipeline implemented in USEARCH (Edgar et al., 2011) processed the bacterial and fungal sequence reads including a quality control and filtering (Frey et al., 2016; Perez-Mon et al., 2020). Paired-end reads were matched with USEARCH (Edgar and Flyvbjerg, 2015), substitution errors were corrected using BayesHammer (Nikolenko et al., 2013), and PCR primers were detected and trimmed using Cutadapt (Martin, 2011), allowing for 1 mismatch and read lengths >300 bp (16S rRNA) and >200 bp (ITS). Sequences were then

dereplicated and removed from singletons. Subsequently, operational taxonomic units (OTUs) were clustered using a threshold of 97% identity with an "on-the-fly" chimera detection algorithm (Edgar, 2013). A Bayesian classifier with 60% as the minimal bootstrap support implemented in MOTHUR (Schloss et al., 2009) was used prior to querying 16S rRNA (Bacteria) and ITS reads (Fungi) against the SILVA v.138.1 (Quast et al., 2013) and UNITE v.8.2 (Kõljalg et al., 2020) reference databases, respectively, to provide the final taxonomical classification of the OTUs detected. We recovered a total of 1,025,452 prokaryotic reads clustered into 5,066 OTUs and 717,020 fungal reads clustered into 1,976 OTUs.

The bacterial and fungal abundance was quantified for three replicates per treatment at 0, 21 and 105 days of recovery using quantitative real-time PCR (qPCR) of the bacterial 16S $rRNA_{V3-V4}$ genomic region (using primer pairs 27F/519r) and fungal ITS2 region (using primer pairs ITS3/ITS4). An amount of 6.6 µL of diluted DNA from the extraction was added to 7.5 µL of SYBR™ Green PCR master mix solution, 0.5 µL of HPLC Water, 0.1 µL of BSA, and 0.15 µL of each primer (the same primers as for the amplicon sequencing without the barcodes). An amount of 15 µL of DNA master mix solution was added to an ABI7500 Fast Real-Time PCR system (Applied Biosystems, Foster City, United States). The qPCR was initiated at 95°C for 15 min, followed by 40 amplification cycles (each at 95°C for 30 s, 90°C for 45 s and 72°C for 45 s) and a subsequent melting curve (at 95°C for 15 s, 60°C for 60 s and 95°C for 15 s). The standard curves (three for each targeted region) were obtained from a tenfold serial dilution (10^{-1} to 10^{-9} copies) of plasmids generated from cloned targets. The bacterial and fungal abundance as the number of cell copies was related to the total DNA in the sample (ng µL^{-1}) and the DW of the sample (g DW) to obtain cells g DW^{-1}.

Autotrophic community analysis

The community structure of the photoautotrophic organisms (hereafter referred to as autotrophic) was determined in three replicates per treatment at 0, 21 and 161 days of recovery. Autotrophs were extracted from the sediments (13.4 ± 6.6 g DW) following the protocol of Mendoza-Lera et al. (2017). In short, after adding 30 mL deionized water, each sample was vortexed at a maximum velocity for 1 min (Janke and Kunkel, Germany) and sonicated at a low intensity for 5 min (Bandelin Sonorex, Germany). A subsample of 100 µL or 200 µL of the supernatant, depending on the concentration of autotrophs and particles, was placed in an Utermöhl chamber (∅ = 25.8 ± 0.19 mm, Hydrobios, Germany), stained with the same volume of Bengalrosa and left to settle overnight before counting the living diatoms (cells or frustules with chloroplasts), empty diatoms (cells or frustules without any chloroplast), chlorophytes and cyanobacteria. Approximately 400 living cells were enumerated at a magnification of 400x using an inverse light microscope (Axioskop2, Zeiss, Germany). Living diatoms and cyanobacteria were grouped by morphotype (Streble and Krauter, 1988; Cox, 1996; von Berg et al., 2012) using their morphology and length (according to the longest axis). The abundance of each morphotype is related to the DW of the sediment (cells g DW^{-1}) in the sample. The autotrophic community was composed of living diatoms (50.8%), empty diatom frustules (47.6%) and cyanobacteria (1.9%; values are mean over all replicates, sediment types and sampling dates, $n = 27$). Chlorophytes were not observed in any sample. Trends found

between sediment types during recovery were mainly driven by living diatoms due to the low abundance of cyanobacteria. Therefore, we focused our analysis on the community structure of living diatom morphotypes. The total diatom abundance was calculated as the sum of living diatom cells of each morphotype per sample.

We used Chl a as a measure of autotrophic biomass. Chl a was extracted from wet sediments (1.8 ± 0.5 g DW for days 0 to 42, or 13.6 ± 3.7 g DW for days 105 to 224) with 90% ethanol followed by several cycles of freezing and thawing. After extraction, the Chl a concentration was measured by high-performance liquid chromatography (Ultimate3000, Thermo Fisher Scientific Corporation, Waltham, MA, United States) and related to the DW of each sample (Scheidweiler et al., 2021).

Statistical analyses

All statistical analyses were performed in the R statistical environment (version 4.1.1, R Core Team, 2021) and considered significant at $p < 0.05$. We tested the interaction of sediment type (dried, migrated, control) and sampling day (0, 4, 7, 21, 42, 105, 161, 224 days) in separate linear models on each response variable (CR, GPP, EEA, Chl a and abundance: diatom cells, 16S and ITS gene copies) via two-way permutation tests (permANOVA, 9,999 permutations) using the *aovp* function of the package *lmPerm* (Wheeler and Torchiano, 2016). Pairwise comparisons between sediment types were implemented for each sampling day as *post hoc* tests by calculating estimated marginal means using the *emmeans* function of the package *emmeans* (Lenth et al., 2023).

We ran a non-metric multidimensional scaling (NMDS) based on a Bray-Curtis distance matrix created by the function *metaMDS* in the *vegan* package (Oksanen et al., 2022) to assess the community structure (β-diversity) of bacteria, fungi and diatoms and fitted functional parameters (CR, GPP, EEA) as gradients via the *envfit* function (*vegan* package, Oksanen et al., 2022) to the NMDS. We performed permutational multivariate analyses of variance (PERMANOVA, 9,999 permutations, Bray–Curtis dissimilarity) separately for each sampling day using the function *adonis* (*vegan* package, Oksanen et al., 2022). Mantel tests (9,999 permutations, Spearman correlations) were performed using the function *mantel* in *vegan* (Oksanen et al., 2022) in order to test for correlations between community function (Euclidean distances, including CR, GPP and EEA) and structure (Bray Curtis distances) on each sampling day. All data were scaled to values between zero and one before the analyses.

We also calculated principal response curves (PRC) *sensu* van Den Brink and Ter Braak (1999) to assess the community response to the effect of the stress (dried and migrated) relative to the control at each specific time point. This has the advantage of partialling out the effect of a changing control over time due to seasonal effects. Instead, a basic response pattern of the entire community is modeled for each sediment type and displayed by a response score (y-axis). The response scores are based on the first axis of a distance-based redundancy analysis (Bray-Curtis distance) and were calculated by the function *capscale* (package *vegan*; Oksanen et al., 2022), with the sediment type as the explanatory variable and recovery time as a covariable. As the control is set to zero, deviations of the x-axis can be seen as a sediment-type-related community response. Secondly, species weights display

taxon-specific affinity to the overall community response, meaning that species with high positive or negative weights correspond most to the response of the respective sediment type. Small or zero species scores indicate that the individual species reaction differs from the community response (but does not exclude a general response to the sediment type, see van Den Brink and Ter Braak, 1999). Additionally, the sign of the species weights determines the direction (an increase or decrease in abundance) of the species depending on the sign of the community response. The proportional change in abundance (relative to the control) at a specific time point can be calculated by exp (sediment type score * species weight). The fitness of the PRC was tested by an analysis of variance (ANOVA) on the first axis [bacteria: $F(1,18) = 18.77$, $p < 0.001$; fungi: $F(1,18) = 13.66$, $p = 0.001$, diatoms: $F(1,18) = 7.73$, $p = 0.011$], following Graeber et al. (2017), showing that all PRCs significantly explained the data.

Results

Environmental parameters

DOC in the river water varied between 3.65 and 4.87 mg L^{-1} and dissolved inorganic nitrogen (DIN: sum of NO$_3$-N, NO$_2$-N and NH$_4$-N) ranged between 0.92 and 2.95 mg L^{-1} with no seasonal trend (Supplementary Table S1). SRP was highest in the winter (up to 21.3 ± 0.6 µg L^{-1} in December at day 42) and lowest in early spring (3.2 ± 0.4 µg L^{-1} in February at day 105 and in April at day 161). The low SRP concentration in early spring caused the high DIN:SRP ratio of 264–442 during this period. The DIN:SRP ratio estimated 56 at all other sampling dates (Supplementary Table S1).

Community respiration and gross primary production

The initial mean CR for stressed sediments was 0.36 ± 0.25 µgO$_2$ h^{-1} gDW^{-1} (dried) and 1.46 ± 0.05 µgO$_2$ h^{-1} gDW^{-1} (migrated) and, thus, significantly lower than the control (3.46 ± 0.35 µgO$_2$ h^{-1} gDW^{-1}, $p < 0.001$, Supplementary Table S2). CR was marked by a sharp increase within the first 3 weeks (Figure 1A). The dried sediments showed a steeper response to the stress relief (6.5-fold increase) than migrated sediments (1.5-fold increase). CR of stressed sediments was different from the control at day 4 ($p < 0.001$) and partially at day 7 (dried: $p = 0.012$, migrated: $p = 0.08$). At day 21, both sediments had recovered to the level of the control (dried: $p = 0.677$, migrated: $p = 0.342$, Figure 1A). CR remained constant at 2.92 ± 0.81 µgO$_2$ h^{-1} gDW^{-1} (dried) and 3.22 ± 0.98 µgO$_2$ h^{-1} gDW^{-1} (migrated) until day 224, being similar to the control (3.57 ± 0.93 µgO$_2$ h^{-1} gDW^{-1}).

A fast resumption of metabolic activity could be observed for CR, however, the recovery of GPP from drying and migrating was much slower (Figure 1B). GPP started at 0.13 ± 0.17 µgO$_2$ h^{-1} gDW^{-1} (dried) and 2.38 ± 0.41 µgO$_2$ h^{-1} gDW^{-1} (migrated) compared to 6.29 ± 0.64 µgO$_2$ h^{-1} gDW^{-1} of the control, proving a significant difference ($p < 0.001$). Dried sediments showed a steady increase in GPP within the first 3 weeks with a 27.7-fold increase from the initial activity to 3.72 ± 0.43 µgO$_2$ h^{-1} gDW^{-1}, but rapidly declined to 1.14 ± 0.30 µgO$_2$ h^{-1} gDW^{-1} at day 42 (Figure 1B). By contrast, migrated sediments provided only a 1.9-fold increase of GPP within 7 days to 4.64 ± 3.00

µgO$_2$ h^{-1} gDW^{-1}, before also dropping to 1.56 ± 0.83 µgO$_2$ h^{-1} gDW^{-1} at day 42. We found significant differences in GPP between stressed sediments and the control until day 161 ($p < 0.05$, Supplementary Table S2) except for dried sediments at day 21 ($p = 0.201$) and migrated sediments at day 42 ($p = 0.998$) and day 105 ($p = 0.685$). GPP of stressed sediments recovered to similar rates as the control at day 224 (dried: 5.36 ± 0.86 µgO$_2$ h^{-1} gDW^{-1}, migrated: 4.61 ± 0.41 µgO$_2$ h^{-1} gDW^{-1}, control: 6.48 ± 1.57 µgO$_2$ h^{-1} gDW^{-1}).

Based on the ratio of GPP to CR (GPP:CR), dried sediments started the recovery process net heterotrophic (GPP:CR = 0.34 ± 0.28), whereas migrated sediments were net autotrophic (1.63 ± 0.23), similar to the control (1.84 ± 0.30, Supplementary Figure S3). GPP:CR ratio decreased in all sediments to a seasonal minimum in December (day 42), with the control remaining autotrophic (1.03 ± 0.21) and both dried (0.43 ± 0.06) and migrated sediments (0.46 ± 0.20) changing to net heterotrophy. The stressed sediments remained net heterotrophic until day 161 of recovery and returned to the control level at day 224.

Potential extracellular enzyme activities

Most C-acquiring enzymes (BG, PO, PP) were not significantly different among treatments (Supplementary Table S2). However, the potential activity of AP (P-acquiring) and LAP (N-acquiring) matched the general trend of increasing CR with ongoing recovery (Figure 2). The potential activity of BX was always below the limit of detection. Migrated sediments showed especially low initial potential activity for BG, NAG, AP, LAP and PO (max. 27.3% of the control values). By contrast, NAG, AP and LAP had low potential activities in dried sediments (up to 18.4%), but the potential activity of BG was surprisingly high (57.9% of the control) and PO even exceeded the control (121.7%). AP activity was significantly different from the control for both sediment types until day 21 (dried: $p = 0.007$, migrated: 0.011). All potential enzyme activities but that of AP increased within 3 weeks (21 days) and were comparable to the control (Figure 2). Related to the control, AP was the only enzyme to remain at a significantly low potential activity at 35.9% (dried) and 32.0% (migrated) of the control even at day 21 (Figure 2).

Bacterial, fungal and diatom community structure

The bacterial community was clearly structured according to the sediment type [Day 0: $F(2,8) = 10.13$, $p = 0.004$; Day 21: $F(2,8) = 6.38$, $p = 0.004$; Day 105: $F(2,8) = 5.05$, $p = 0.004$] and recovery time (Supplementary Figure S4A). The largest variability concerning temporal development was observed in the bacterial community of dried sediments, whereas migrated sediments showed a less pronounced community change over time. The PRC presented a strong community effect of the sediment type for dried sediments ($p < 0.05$), which intensified with ongoing recovery and did not indicate a return to the control at the end of the experiment (Figure 3A). *Flavobacterium* was correlated strongest with the community response of dried sediments (1.6-fold increased abundance compared to control), whereas several *Oxyphotobacteriae* (phylum Cyanobacteria) had a reduced abundance at all points in
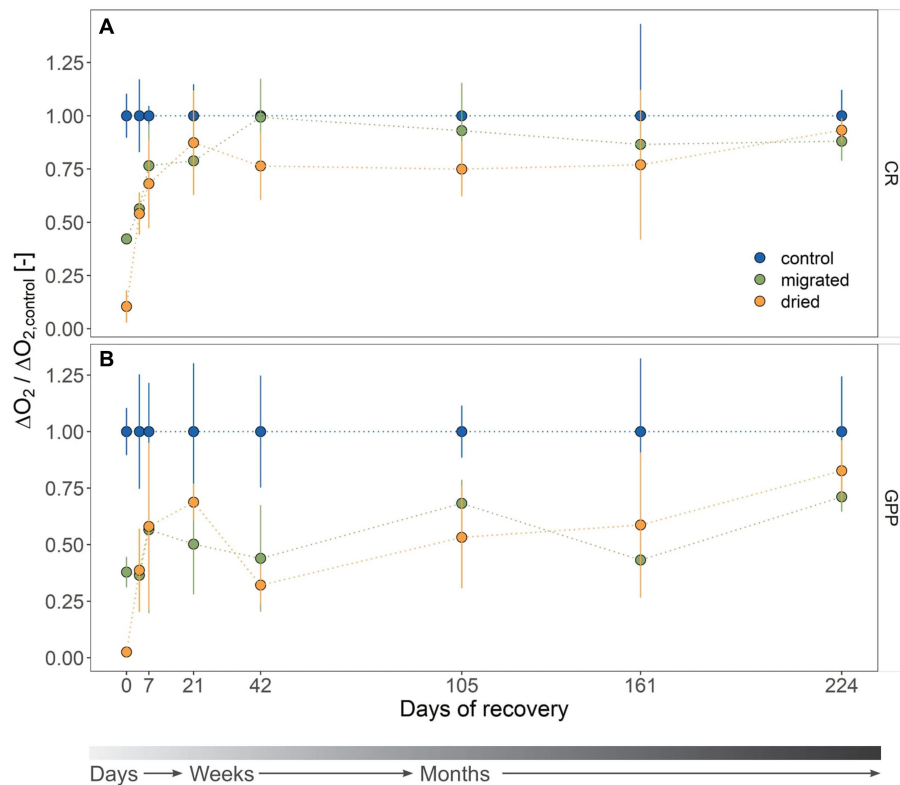
FIGURE 1
Metabolic activity of the microbial community associated with sandy sediments as community respiration (CR, **A**) and gross primary production (GPP, **B**) during the recovery (mean±standard deviation, $n=4$). Sediment type is indicated by color. Rates are microbial consumption (CR, $\Delta O_2<0$) or production (GPP, $\Delta O_2>0$) of dissolved oxygen (DO) related to sediment dry weight (DW; µg O_2 h^{-1} g DW^{-1}). All rates are standardized to the mean rate of the control, yielding a dimensionless ratio. The gray color gradient bar helps to visualize the temporal scale of the recovery.

recovery (an average of 69% of the control). The bacterial community in migrated sediments showed no community response, and species abundances only marginally increased or decreased relative to the control during the entire observation period (Figure 3A).

The fungal community structure was significantly impacted by sediment type at the start of recovery [$F(2,8)=13.66$, $p=0.004$] and approached the control toward longer recovery time [Day 21: $F(2,8)=1.82$, $p=0.088$; Day 105: $F(2,8)=1.31$, $p=0.187$]. Fungal community structure in dried sediments showed a similar large variability between replicates as the bacteria community, especially at day 21 (Supplementary Figure S4B). At the same time, the fungal community was comparable among migrated sediments and the control already at day 21 (Supplementary Figure S4B). The PRC demonstrated a strong sediment-type-related community response for dried sediments in the beginning, which attenuated toward longer recovery (Figure 3B). *Alternaria sp.* had the highest negative species weight at the start of recovery and showed a 22.9-fold increased abundance in dried sediments relative to the control. *Aureobasidium pullulans* accounted for the second strongest correlation to the overall community response (7.5-fold abundance compared to control). Several unclassified fungi showed a contradictory behavior by having positive species weights and, therefore, a reduced abundance in dried sediments (e.g., a minimum of 32% of the control at the start of recovery). Similar to the bacterial community response, the fungal response in migrated sediments had a smaller range than in dried sediments. The fungal community in migrated sediments, showing

little or no overall response at the start of recovery, responded only very slightly at the end of recovery (Figure 3B), with *Alternaria sp.* being the species with the highest deviation from the control (1.6-fold increased abundance). When looking at relative abundance, Dothideomycetes were initially the most dominant fungal group in dried sediments (in concordance with Schreckinger et al., 2021), but their relative abundance decreased with increasing recovery time (Supplementary Figure S5).

The diatom community was dominated by small-sized morphotypes with a length of <50 µm (44.8%) and 50–100 µm (19.8%). The diatom community structure of migrated and dried sediments differed significantly from the control at the start of recovery [$F(2,7)=9.99$, $p=0.004$] and was unaffected by sediment type thereafter [Day 21: $F(2,9)=1.53$, $p=0.203$; Day 161: $F(2,8)=1.58$, $p=0.205$]. The PRC, despite high variabilities in all sediments depending on recovery time, revealed a strong sediment-type-related response, especially in migrated sediments (Figure 3C). All diatom morphotypes were negatively affected by the two stresses (showing negative species weights), with *Navicula* occurring only up to 7.9% in migrated sediments relative to the control (in dried sediments: 27.5%), followed by *Fragilaria* (migrated: 22.4%, dried: 46.8%) and *Achnanthes* (migrated: 35.1%, dried: 58.7%). Although the sediment-type-related PRC score was less pronounced at the end of the experiment, diatom abundances were still reduced and did not return to the control level.

Microbial function (CR, GPP, EEA) was significantly correlated to bacterial (Mantel test, $R^M=0.33$, $p=0.043$), fungal ($R^M=0.30$,
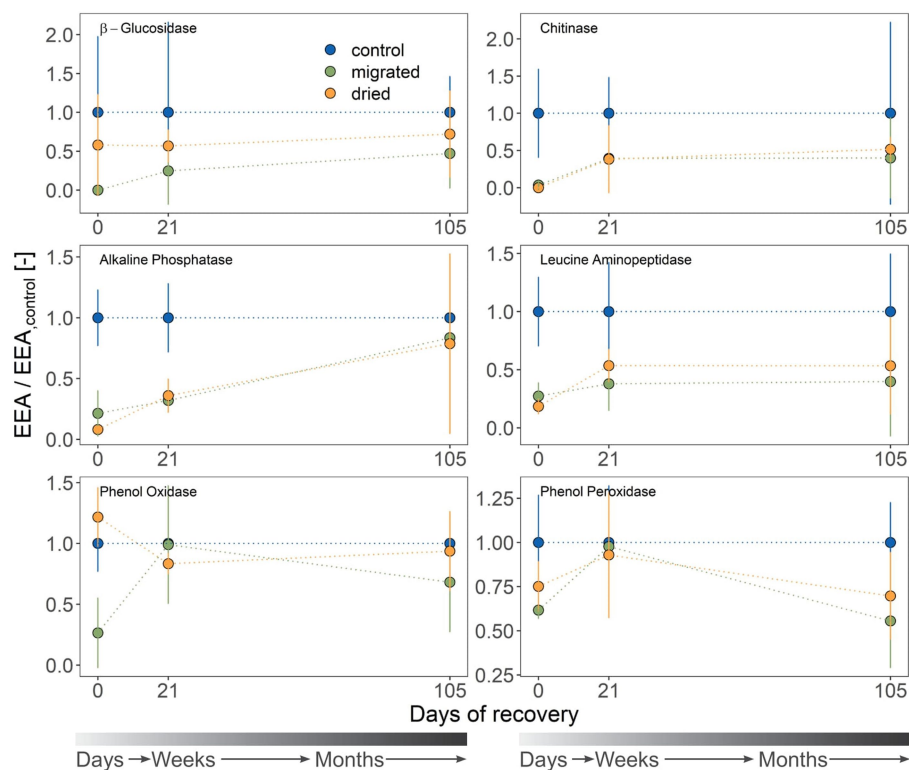
FIGURE 2
Extracellular enzyme activities (EEA; mean±standard deviation, n=3) at three sampling days. Sediment type is indicated by color. β-xylosidase (BX) is not shown due to values being lower than the limit of detection. Activities (µmolmL^{-1} h^{-1}) are standardized to those of the control, yielding a dimensionless ratio. The gray color gradient bar helps to visualize the temporal scale of the recovery.

$p = 0.043$) and diatom community structure ($R^M = 0.46$, $p = 0.025$) at the start of recovery. Thereafter, microbial functions were not related to community structure at day 21 (bacteria: $R^M = -0.17$, $p = 0.783$, fungi: $R^M = -0.05$, $p = 0.560$, diatoms: $R^M = -0.11$, $p = 0.679$) and day 105 (bacteria: $R^M = 0.18$, $p = 0.139$, fungi: $R^M = -0.05$, $p = 0.584$) and day 161 (diatoms: $R^M = -0.11$, $p = 0.695$), respectively.
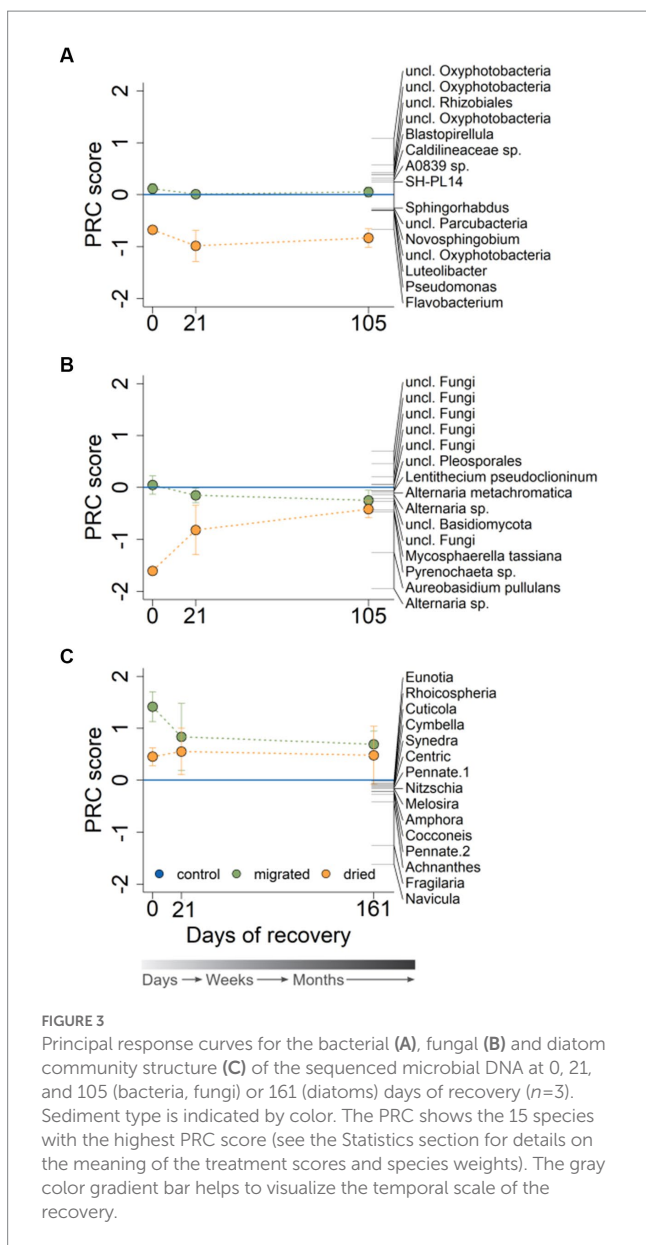
Bacterial, fungal and diatom abundance

Initial bacterial abundances in migrated ($2.65 \pm 2.73 \times 10^8$ gene copies, $p = 0.921$) and dried sediments ($1.08 \pm 0.33 \times 10^8$ gene copies, $p = 0.129$) were comparable to that in control sediments ($3.01 \pm 0.54 \times 10^8$ gene copies, Figure 4A; note the large standard deviation among replicates). Dried sediments had a significantly lower bacterial abundance at day 21 ($1.58 \pm 1.01 \times 10^8$ gene copies, $p < 0.001$) and day 105 ($1.90 \pm 0.78 \times 10^8$ gene copies, $p = 0.036$) compared to the control ($7.09 \pm 1.10 \times 10^8$ gene copies), whereas migrated sediments showed a similar increase in bacterial abundance ($6.51 \pm 1.48 \times 10^8$ gene copies; day 21: $p = 0.673$; day 105: $p = 0.858$) as the control. The fungal abundance was similar in all sediment types and across sampling dates ($1.29 \pm 1.07 \times 10^8$ gene copies, Figure 4B) with the exception of significantly lower abundance in dried sediments at day 105 ($0.56 \pm 0.39 \times 10^8$ gene copies, $p = 0.01$).

The initial diatom abundance was 3.8-fold higher in dried ($3.99 \pm 0.34 \times 10^5$ cells gDW^{-1}) than in migrated sediments ($1.04 \pm 0.31 \times 10^5$ cells gDW^{-1}), but only their abundance in migrated sediments

was significantly lower than the control ($1.30 \pm 1.36 \times 10^6$ cells gDW^{-1}, $p = 0.022$, Figure 4C). Within 3 weeks of recovery, the diatom abundance of stressed sediments was comparable to that of the control ($2.14 \pm 1.44 \times 10^5$ cells gDW^{-1}, dried: $p = 0.951$, migrated: $p = 0.902$). Similar to diatom abundance trends, dried sediments (0.44 ± 0.02 µgChla gDW^{-1}) had initially a 2.8-fold higher Chl a concentration than migrated sediments (0.15 ± 0.02 µgChla gDW^{-1}, $p = 0.001$), both significantly ranging below the initial Chl a concentration in control sediments (1.20 ± 0.13 µgChla gDW^{-1}, $p < 0.001$, Figure 4D). The Chl a increased in both dried and migrated sediments and recovered to concentrations of the control within 7 days (dried: $p = 0.993$, migrated: $p = 0.574$). For the remaining months, Chl a in dried and migrated sediments was comparable to the control and increased in all sediments until day 224 (Figure 4D). Unlike dried sediments (0.47 ± 0.17 µgChla gDW^{-1}, $p = 0.323$), migrated sediments showed a significantly lower Chl a concentration here (0.25 ± 0.08 µgChla gDW^{-1}, $p < 0.001$) compared to control sediments (0.56 ± 0.19 µgChla gDW^{-1}).

Influence of mesh bags on the seasonality of functional and structural parameters

In situ sediments showed little seasonal fluctuations of CR (3.94 ± 1.45 µgO$_2$ h^{-1} gDW^{-1}, $n = 28$) and GPP (7.45 ± 1.05 µgO$_2$ h^{-1} gDW^{-1}, $n = 28$) over the course of our experiment, with the exception of a peak in early spring (CR: 10.06 ± 4.29 µgO$_2$ h^{-1} gDW^{-1}; GPP:

FIGURE 3
Principal response curves for the bacterial **(A)**, fungal **(B)** and diatom community structure **(C)** of the sequenced microbial DNA at 0, 21, and 105 (bacteria, fungi) or 161 (diatoms) days of recovery (*n*=3). Sediment type is indicated by color. The PRC shows the 15 species with the highest PRC score (see the Statistics section for details on the meaning of the treatment scores and species weights). The gray color gradient bar helps to visualize the temporal scale of the recovery.
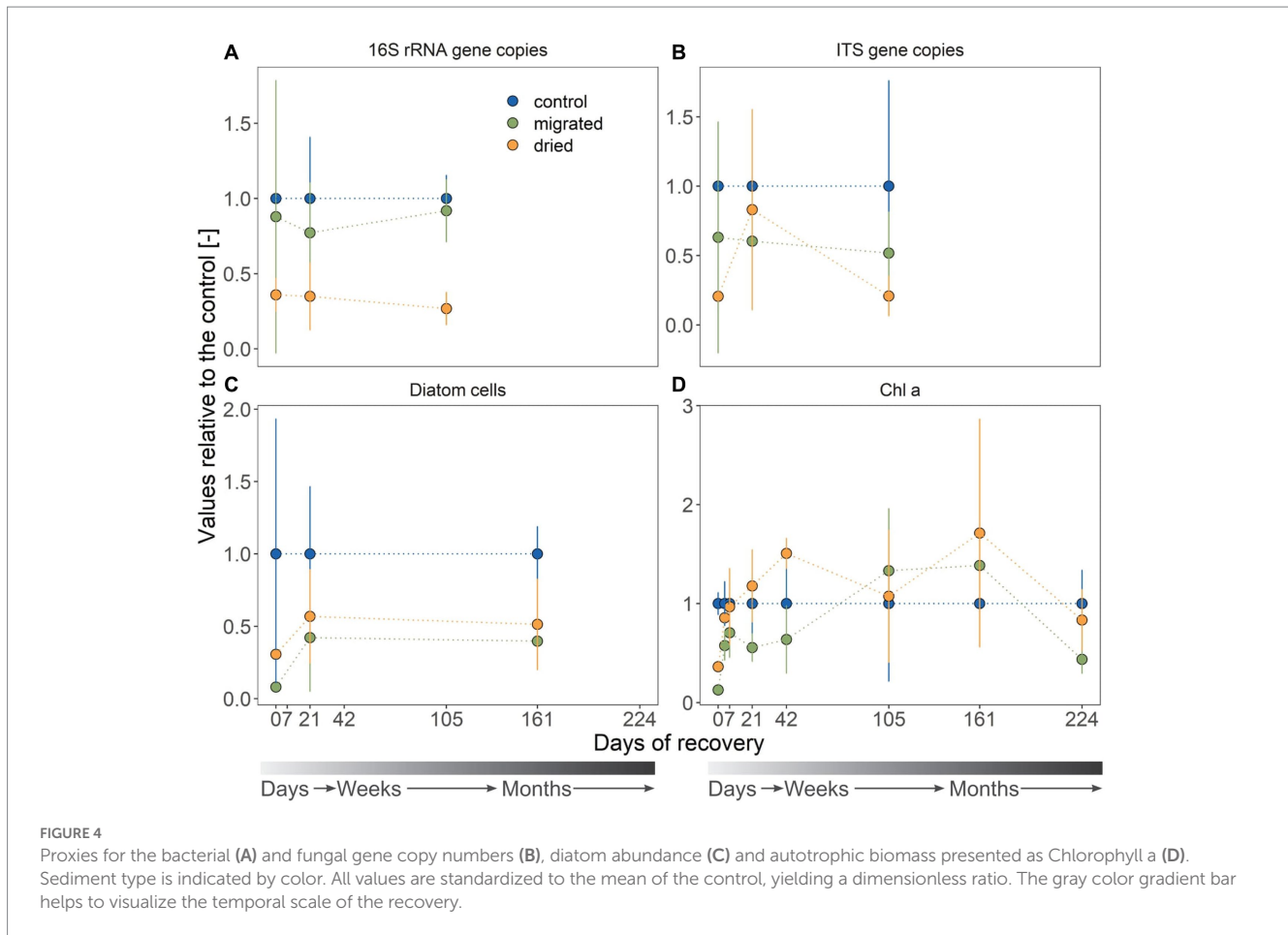
Discussion

Long-term impacts of sediment drying (severe episodic stress) and bedform migration (moderate periodic stress) have been largely overlooked in the research on riverbed microbial communities. Our experimental study shows that the response of the microbial community was not limited to the immediate stress release, but persisted for several months. The short durations of many published experimental studies (e.g., McKew et al., 2011; Truchy et al., 2020) might therefore not cover the time required for full microbial community recovery. Investigations of long-term recovery in the range of months inevitably overlap with seasonal variations, such as discharge, temperature, light and nutrient supply. Although both stressed sediments paralleled the seasonal fluctuations of *in situ* and control sediments (e.g., GPP:CR ratio, Supplementary Figure S1, and Chl a dynamics, Supplementary Figure S6), their long-term recovery superimposed these natural seasonal variations. The seasonal fluctuations of the control sediments in our mesh bags and the *in situ* sediments were comparable, indicating that the conditions in the mesh bags mirrored the natural environment of the microbial communities in the riverbed despite lower light availability.

Microbial communities were stressed by sediment drying and bedform migration

To the best of our knowledge, this is the first study comparing the response of microbial communities to sediment drying and immobilization. Both sediment drying and migration led to reduced CR and GPP, potential activities of P- (AP) and N-acquiring (LAP) enzymes, autotrophic and heterotrophic abundances, and diverging community structure at the beginning of recovery. Sediment drying (Acuña et al., 2005; Corcoll et al., 2015; Goldman et al., 2017) and bedform migration (Zlatanović et al., 2017; Scheidweiler et al., 2021) are described as suppressing community metabolism, pointing to the limited resistance of the microbial community function (Allison and Martiny, 2008). Decreasing enzyme activity as a result of drying slows down the degradation of organic matter (Amalfitano et al., 2008; Gionchetta et al., 2019), whereas sediment migration dislocates enzymatic activity from the top and mobile layer toward deeper and immobile sediment layers (Atkinson et al., 2008).

As expected, the initial bacterial community structure in dried sediments differed considerably from the control, whereas the effect of bedform migration did not stand out as clearly. The sediment drying involved a shift in the bacterial community structure which is comparable to other studies (Rees et al., 2006; Fazi et al., 2013; Calapez et al., 2014). The fungal community structure in dried sediments, similar to the bacterial community structure, diverged from the control. The detrimental effects of sediment drying on numerous aquatic fungi are shown by the decreasing abundance of several unclassified fungi. Classified species with increased abundance were *Flavobacterium*, *Alternaria* sp. and *Aureobasidium pullulans*. The latter, a yeast-like fungus, is known for its adaptive phenotypic plasticity and ability to colonize extreme environments worldwide (Gostinĉar et al., 2012; Xiao et al., 2019). The high content of osmoregulative

21.26 ± 6.77 μgO$_2$ h^{-1} gDW^{-1}, *n*=4, Supplementary Figure S6). Compared to *in situ* sediments, the control sediments in mesh bags tended to have slightly lower microbial activity and abundances, especially in autotrophic parameters (Chl a, GPP:CR ratio) and in times of high biomass productivity (spring). The most notable discrepancy between *in situ* sediments and control sediments in mesh bags was observed at day 105 of recovery (February) when *in situ* sediments exceeded mesh bags in most parameters, particularly in CR and GPP (Supplementary Figures S6–S8). The control sediments in mesh bags and the *in situ* control had a comparable amount of organic matter independent of the sampling date (*p*=0.83, data not shown). The mesh size (250 μm) is a commonly used pore size for microbial decomposition processes, e.g., in leaf litter decomposition experiments (Lecerf, 2017; Gossiaux et al., 2019; Zhai et al., 2019). We conclude that the mesh bag seemed to have dampened seasonal amplitudes in most parameters of metabolism and abundance, but mirrored overall seasonal fluctuations proportionally.

FIGURE 4
Proxies for the bacterial **(A)** and fungal gene copy numbers **(B)**, diatom abundance **(C)** and autotrophic biomass presented as Chlorophyll a **(D)**. Sediment type is indicated by color. All values are standardized to the mean of the control, yielding a dimensionless ratio. The gray color gradient bar helps to visualize the temporal scale of the recovery.

aquaporins (Gostinĉar et al., 2012) and the accumulation of melanin, a protective dark pigment in fungal cell walls, are assumed to contribute to its drought resistance (Gostinĉar et al., 2012). Thus, the ability of specific fungi species to cope with drying could explain the realignment of fungal communities from dried and control sediments within 21 days.

In contrast to heterotrophs, the autotrophic community structure was affected by both sediment drying and bedform migration. The abundance of the dominant diatom morphotypes *Navicula*, *Fragilaria* and *Achnanthes* was initially about one order of magnitude lower in stressed sediments compared to the control. Diatom frustules suffer mechanical damage when colliding with mobile sand grains and their habitable area is thus reduced to the fissures and crevices of sand grains (Miller et al., 1987; Delgado et al., 1991). In addition, microbes are perpetually buried beneath depositing grains in migrating bedforms. The resulting light reduction seemed to have a stronger effect on the autotrophic community than on the heterotrophic community (Wilkes et al., 2019). Diatoms are known to be particularly sensitive to drought (Romaní et al., 2013; Piano et al., 2017) and in dried sediments the community is characterized only by a few abundant and dominant taxa (Mathooko et al., 2005), similar to our observations. Yet, their physiology (i.e., r-selected traits, short generation times) facilitates quick recovery upon stress relief if environmental conditions allow (Ledger et al., 2013; Calapez et al., 2014; Barthès et al., 2015).

Heterotrophic processes dominated during recovery

The benthic microbial communities responded to the relief from stress by immediately increasing their metabolic activity until full functional recovery within 8 months. The potential EEA of both types of stressed sediments reached activities of the control after only 3 weeks of recovery (except for aminopeptidase and phosphatase). This result is consistent with the EEA recovery (10–14 days) observed following stream rewetting after 13 weeks of drying (Pohlon et al., 2013). The recovering bacterial community is described as having a high need for C, N, and P, which, in turn, fuels the synthesis of related enzymes (Ylla et al., 2010). Thus, our results highlight that the accumulated resources during sediment drying and migration are quickly metabolized by EEA upon rewetting and immobilization, respectively. These results support our first hypothesis, illustrating that microbial communities in temperate riverbeds recover functionally from previous stresses irrespective of the stressor type, and match reported positive short-term recovery trends from drying and migrating (Marxsen et al., 2010; Pohlon et al., 2013; Oprei et al., 2019).

The time required for full recovery of autotrophic activity (GPP, more than 5 months) exceeded that for heterotrophic activity (CR, less than 7 days), which explains the shift toward heterotrophy as suggested in past studies (Timoner et al., 2012; Veach et al., 2016; Colls et al., 2019). Both dried and migrated sediments were net heterotrophic between 6 weeks and 4 months of recovery (December

to February). By contrast, the control remained net autotrophic even during the light-limited winter months. Low EEA potentials are also known to correlate with the heterotrophic dominance in microbial communities (Romaní and Sabater, 2000), matching our observations of net heterotrophy during recovery. Hence, both drying and migrating caused a long-lasting shift toward net heterotrophy. Both stresses had a minor effect on heterotrophs (i.e., bacterial and fungal abundances), while autotrophs (i.e., Chl a and the abundance of diatoms) were clearly affected. Autotrophs are described to be more resilient to drying, whereas heterotrophs are known to be more resistant (Timoner et al., 2012; Acuña et al., 2015). The comparable bacterial and fungal abundances between stressed and control sediments could be related to methodological constraints. We used qPCR to quantify bacteria and fungi that replicate all DNA in a sample. Therefore, it is possible that a fraction of gene copies counted in stressed sediments was actually from inactive cells (dead or spore) falsely indicating heterotrophic resistance.

Although CR and GPP are a reliable and well-established measure of overall ecosystem metabolism (Fellows et al., 2006; del Giorgio and Williams, 2008; Young et al., 2008), this method has the fallback of being a "black box" approach for microbial function. Integrating molecular approaches such as metatranscriptomics, metaproteomics and metabolomics, might deepen our understanding of individual processes, transformations and functional recovery on the micro- and nanoscale (Mapelli et al., 2008; Jansson et al., 2012; Franzosa et al., 2015; Biswas and Sarkar, 2018).

Functional recovery is decoupled from structural recovery

Our results imply a partial decoupling between functional and structural recovery in microbial communities based on Mantel test results, which confirm our second hypothesis. The probably light-limited, seasonally induced decrease in Chl a contrasted with the increase of GPP during the first 3 weeks of recovery and points to a decoupling of primary production and autotroph biomass, as it has already been observed in migrating sediments (Scheidweiler et al., 2021) and lentic sediments after nutrient enrichment (McCormick et al., 2019). Despite the decoupling observed between GPP and Chl a, the long time needed for GPP recovery coincided with the diminished population of some dominant diatom morphotypes, for example, *Navicula* and *Fragilaria*. Past studies highlighted that the abundance of individual taxa can be proportional or disproportional to their contribution to the ecosystem metabolism, and suggest that functional traits of individual species play a bigger role in microbial metabolism than overall community structure (Han and Furuya, 2000; McCormick et al., 2019).

In contrast to the strictly negatively affected diatoms, the heterotrophic community was characterized by both positive and negative PRC species weights and showed distinct community structure during recovery. Although poorly resistant microbial communities are often prone to an alteration after undergoing a stress period (Allison and Martiny, 2008), ecological processes may be restored at the community level due to multifaceted functional redundancy and metabolic plasticity (Comte et al., 2013; Woodward et al., 2015; Louca et al., 2018). The functional gene pool in microbial

communities with contrasting taxonomic compositions, for example, was found to be similar (Burke et al., 2011; Dopheide et al., 2015), enabling the quick resumption of viable functions after stress despite lacking structural resilience (Barthès et al., 2015). In our experiment, this held true for CR and most EEA (full recovery within 3 weeks), but not for GPP.

Findings from recent studies have challenged the concept of functional redundancy in microbiology, as high structural biodiversity correlates with multifunctionality and a broad diversity of metabolic pathways (Peter et al., 2011; Galand et al., 2018) and increases community resistance to stress (Steudel et al., 2012; Feng et al., 2017). In turn, reduced trophic complexity in microbial communities provoked by loss of species engenders a decrease in community function (Santschi et al., 2018). Thus, the long recovery time for GPP in our study could have been a secondary consequence of the strictly negative effects of drying and bedform migration on autotrophic abundance and community structure seen in the PRC. In contrast, bacterial and fungal abundance was characterized by both positive and negative changes driven by sediment type and individual species. Therefore, the heterogeneity in bacterial and fungal stress response points to a partial disentanglement of metabolic function and heterotrophic community structure (Langenheder et al., 2005) and probably facilitated the fast recovery of CR at the community level.

Stressor type shapes long-term structural but not functional recovery

Benthic heterotrophic communities that experienced drying initially showed a stronger structural response than those that experienced bedform migration. This result indicates that episodic drying had a more devastating impact on the heterotrophic microbial community than periodic bedform migration. Our results endorse former observations that the microbial reaction is linked to the previous stress intensity (Berga et al., 2012). Apart from the immediate short-term recovery, the stressor type had no further impact on the long-term recovery of microbial function, therefore, partly rejecting our third hypothesis. Our results suggest that the type and severity of stress shapes the functional recovery shortly after the relief from stress, but this regulative effect does not persist in the long-term. The parallel development of microbial function, being irrespective of the previous stressor type, builds on a deterministic succession of bacterial communities (driven by abiotic environment, i.e., nutrient supply, substrate availability, chemical properties) on a functional level (Veach et al., 2016). Therefore, when formerly distinct communities (i.e., from dried and migrated sediments) are placed into a similar environment (i.e., rewetted and immobilized), their functional services will converge in the long-term.

Opposed to community function, the stress type had longer-lasting effects on the microbial community structure, which is in line with our third hypothesis. We infer this behavior from secondary successional dynamics following a stress-induced degeneration of a mature community (Kearns and Shade, 2018). Post-stress colonization occurs through both resistant local taxa inhabiting the stressed sediments, as well as immigrating regional taxa from the surrounding water column and neighboring habitats (Folke et al., 2004; Kearns and Shade, 2018).

However, the convergence of communities was not reached in the timescale of our experiment, as the structures of the bacterial (except migrated sediments), fungal and diatom community were still distinct between stressed and control sediments at 105 and 161 days of recovery, respectively. Our results suggest that the impacts of sediment drying and migrating are not limited to the recovery period observed here, but persist further as a legacy effect that can influence the long-term successional trajectory of community assembly (Andersson et al., 2014; Hawkes and Keitt, 2015; Vass and Langenheder, 2017). Most microbial communities in temperate streams are subject to seasonal fluctuations regarding their structural assemblage, abundance and EEA (Wilczek et al., 2005; Hullar et al., 2006; Paruch et al., 2020) and their natural dieback in fall overlaps with the recovery period from summer drying and immobilization observed in our experiment. To the best of our knowledge, the fact that a stress-induced community shift can outlast seasonal variations and may be carried along to the next episodic stress period, acting as a legacy effect and, thus, influencing future responses of the microbial community toward the stress, has not been observed before. Based on our results, it is still unclear whether the microbial community structure in stressed sediments will further approximate that of the control if recovery lasts longer than three and a half months, i.e., if the legacy effect is temporary or permanent.

Importance of recurring stress events

We showed that microbial communities of a riverbed were capable of recovering functionally and structurally from both stressors, i.e., sediment drying and bedform migration. Autotrophic activity (GPP) had a long recovery time (at least 6 months), which was independent of the previous stress type but influenced by seasonal dynamics. By contrast, heterotrophic activity (CR) resumed rapidly subsequent to the stress. The long recovery times observed in our experiment imply that the previous stress type creates a legacy effect on the recovery trajectory in the microbial community structure despite revealing no prolonged impacts on the functional recovery. The time required for microbial recovery that became evident in our study ranges in the temporal scale of seasonally driven variations in benthic community function and structure. Whereas seasonal changes of environmental conditions did not alter the long-term recovery pathway of benthic microbial communities, we argue that the starting point of recovery cannot be uncoupled from the season. Furthermore, the effects of recurring stress periods, repeatedly interrupting the recovery process, are likely to hamper the ongoing structural reorganization of microbial communities and narrow the capacity for resilience, hence, increasing the role of legacy effects in freshwater ecosystems. Future experiments should consider incorporating multiple cross-seasonal stress recovery cycles to account for the seasonal priming of the community reorganization and the closely linked long-term (lagged) stress effects.

Data availability statement

The datasets presented in this study can be found in online repositories. The names of the repository/repositories and accession number(s) can be found at: https://www.ncbi.nlm.nih.gov/bioproject/

PRJNA780103, doi.org/10.1594/PANGAEA.921544 and https://doi.pangaea.de/10.1594/PANGAEA.941237.

Author contributions

AO, JS, MM, and UR-B conceived and planned the experiments. AO, TK, JS, MM, and UR-B carried out the sampling in field. AO and TK conducted the metabolism measurements. UR-B was in charge of analyzing the dissolved carbon and nutrients and autotrophic samples. AO, JS, and AF performed the enzyme activity measurements, extraction of heterotrophic DNA from sediment samples, and analyses of the sequencing data obtained. AO performed the statistical analyses. AO, JS, TK, AF, MM, and UR-B contributed to the interpretation of the results, provided critical feedback, and helped to shape the manuscript. AO took the lead in writing the manuscript. All authors contributed to the article and approved the submitted version.

Funding

Acknowledgments

Conflict of interest

The authors declare that the research was conducted in the absence of any commercial or financial relationships that could be construed as a potential conflict of interest.

Publisher's note

All claims expressed in this article are solely those of the authors and do not necessarily represent those of their affiliated organizations, or those of the publisher, the editors and the reviewers. Any product that may be evaluated in this article, or claim that may be made by its manufacturer, is not guaranteed or endorsed by the publisher.

Supplementary material

The Supplementary material for this article can be found online at: https://www.frontiersin.org/articles/10.3389/fevo.2023.1112519/full#supplementary-material

References

Acuña, V., Casellas, M., Corcoll, N., Timoner, X., and Sabater, S. (2015). Increasing extent of periods of no flow in intermittent waterways promotes heterotrophy. *Freshw. Biol.* 60, 1810–1823. doi: 10.1111/fwb.12612

Acuña, V., Muñoz, I., Giorgi, A., Omella, M., Sabater, F., and Sabater, S. (2005). Drought and postdrought recovery cycles in an intermittent Mediterranean stream: structural and functional aspects. *J. N. Am. Benthol. Soc.* 24, 919–933. doi: 10.1899/04-078.1

Ahmerkamp, S., Winter, C., Janssen, F., Kuypers, M. M. M., and Holtappels, M. (2015). The impact of bedform migration on benthic oxygen fluxes. *J. Geophys. Res. Biogeo.* 120, 2229–2242. doi: 10.1002/2015JG003106

Allison, S. D., and Martiny, J. B. H. (2008). Resistance, resilience, and redundancy in microbial communities. *Proc. Natl. Acad. Sci. U. S. A.* 105, 11512–11519. doi: 10.1073/pnas.0801925105

Amalfitano, S., Fazi, S., Zoppini, A., Barra Caracciolo, A., Grenni, P., and Puddu, A. (2008). Responses of benthic bacteria to experimental drying in sediments from Mediterranean temporary rivers. *Microb. Ecol.* 55, 270–279. doi: 10.1007/s00248-007-9274-6

Andersson, M. G. I., Berga, M., Lindström, E. S., and Langenheder, S. (2014). The spatial structure of bacterial communities is influenced by historical environmental conditions. *Ecology* 95, 1134–1140. doi: 10.1890/13-1300.1

Atkinson, B. L., Grace, M. R., Hart, B. T., and Vanderkruk, K. E. N. (2008). Sediment instability affects the rate and location of primary production and respiration in a sand-bed stream. *J. N. Am. Benthol. Soc.* 27, 581–592. doi: 10.1899/07-143.1

Aufdenkampe, A. K., Mayorga, E., Raymond, P. A., Melack, J. M., Doney, S. C., Alin, S. R., et al. (2011). Riverine coupling of biogeochemical cycles between land, oceans, and atmosphere. *Front. Ecol. Environ.* 9, 53–60. doi: 10.1890/100014

Baattrup-Pedersen, A., Graeber, D., Kallestrup, H., Guo, K., Rasmussen, J. J., Larsen, S. E., et al. (2020). Effects of low flow and co-occurring stressors on structural and functional characteristics of the benthic biofilm in small streams. *Sci. Total Environ.* 733:139331. doi: 10.1016/j.scitotenv.2020.139331

Barthès, A., Ten-Hage, L., Lamy, A., Rols, J. L., and Leflaive, J. (2015). Resilience of aggregated microbial communities subjected to drought – small-scale studies. *Microb. Ecol.* 70, 9–20. doi: 10.1007/s00248-014-0532-0

Battin, T. J., Besemer, K., Bengtsson, M. M., Romani, A. M., and Packmann, A. I. (2016). The ecology and biogeochemistry of stream biofilms. *Nat. Rev. Microbiol.* 14, 251–263. doi: 10.1038/nrmicro.2016.15

Battin, T. J., Kaplan, L. A., Newbold, J. D., Cheng, X., and Hansen, C. (2003). Effects of current velocity on the nascent architecture of stream microbial biofilms. *Appl. Environ. Microbiol.* 69, 5443–5452. doi: 10.1128/AEM.69.9.5443-5452.2003

Bell, T., Newman, J. A., Silverman, B. W., Turner, S. L., and Lilley, A. K. (2005). The contribution of species richness and composition to bacterial services. *Nature* 436, 1157–1160. doi: 10.1038/nature03891

Belmont, P., Gran, K. B., Schottler, S. P., Wilcock, P. R., Day, S. S., Jennings, C., et al. (2011). Large shift in source of fine sediment in the upper Mississippi River. *Environ. Sci. Technol.* 45, 8804–8810. doi: 10.1021/es2019109

Berga, M., Székely, A. J., and Langenheder, S. (2012). Effects of disturbance intensity and frequency on bacterial community composition and function. *PLoS One* 7:e36959. doi: 10.1371/journal.pone.0036959

Besemer, K. (2015). Biodiversity, community structure and function of biofilms in stream ecosystems. *Res. Microbiol.* 166, 774–781. doi: 10.1016/j.resmic.2015.05.006

Biswas, R., and Sarkar, A. (2018) in *'Omics' tools in soil microbiology: The state of the art*. eds. T. K. Adhya, B. B. Mishra, K. Annapurna, D. K. Verma and U. Kumar, vol. *4* (Singapore: Springer), 35–64.

Bolpagni, R., Laini, A., Mutti, T., Viaroli, P., and Bartoli, M. (2019). Connectivity and habitat typology drive CO 2 and CH 4 fluxes across land–water interfaces in lowland rivers. *Ecohydrology* 12, 1–12. doi: 10.1002/eco.2036

Burke, C., Steinberg, P., Rusch, D., Kjelleberg, S., and Thomas, T. (2011). Bacterial community assembly based on functional genes rather than species. *Proc. Natl. Acad. Sci. U. S. A.* 108, 14288–14293. doi: 10.1073/pnas.1101591108

Burns, A., and Ryder, D. S. (2001). Potential for biofilms as biological indicators in Australian riverine systems. *Ecol. Manage. Restor.* 2, 53–64. doi: 10.1046/j.1442-8903.2001.00069.x

Cabrerizo, M. J., Medina-Sánchez, J. M., Villar-Argaiz, M., and Carrillo, P. (2019). Interplay between resistance and resilience governs the stability of a freshwater microbial food web under multiple stressors. *Sci. Total Environ.* 691, 908–918. doi: 10.1016/j.scitotenv.2019.07.173

Calapez, A. R., Elias, C. L., Almeida, S. F. P., and Feio, M. J. (2014). Extreme drought effects and recovery patterns in the benthic communities of temperate streams. *Limnetica* 33, 281–296. doi: 10.23818/limn.33.22

Cardinale, B. J., Palmer, M. A., Swan, C. M., Brooks, S., and LeRoy Poff, N. (2002). The influence of substrate heterogeneity on biofilm metabolism in a stream ecosystem. *Ecology* 83, 412–422. doi: 10.1890/0012-9658(2002)083[0412:TIOSHO]2.0.CO;2

Charru, F., Andreotti, B., and Claudin, P. (2013). Sand ripples and dunes. *Annu. Rev. Fluid Mech.* 45, 469–493. doi: 10.1146/annurev-fluid-011212-140806

Cole, J. J., Prairie, Y. T., Caraco, N. F., McDowell, W. H., Tranvik, L. J., Striegl, R. G., et al. (2007). Plumbing the global carbon cycle: integrating inland waters into the terrestrial carbon budget. *Ecosystems* 10, 172–185. doi: 10.1007/s10021-006-9013-8

Colls, M., Timoner, X., Font, C., Sabater, S., and Acuña, V. (2019). Effects of duration, frequency, and severity of the non-flow period on stream biofilm metabolism. *Ecosystems* 22, 1393–1405. doi: 10.1007/s10021-019-00345-1

Comte, J., Fauteux, L., and Del Giorgio, P. A. (2013). Links between metabolic plasticity and functional redundancy in freshwater bacterioplankton communities. *Front. Microbiol.* 4, 1–11. doi: 10.3389/fmicb.2013.00112

Corcoll, N., Casellas, M., Huerta, B., Guasch, H., Acuña, V., Rodríguez-Mozaz, S., et al. (2015). Effects of flow intermittency and pharmaceutical exposure on the structure and metabolism of stream biofilms. *Sci. Total Environ.* 503-504, 159–170. doi: 10.1016/j.scitotenv.2014.06.093

Cox, E. J. (1996). *Identification of freshwater diatoms from live material*. London: Chapman & Hall London.

Datry, T., Bonada, N., and Boulton, A. J. (2017). *Intermittent rivers and ephemeral streams: Ecology and management*. Burlington: Elsevier.

del Giorgio, P. A., and Williams, P. J. (2008). Respiration in aquatic ecosystems. *J. Chem. Inf. Model.* 53:287. doi: 10.1017/CBO9781107415324.004

Delgado, M., De Jonge, V. N., and Peletier, H. (1991). Effect of sand movement on the growth of benthic diatoms. *J. Exp. Mar. Biol. Ecol.* 145, 221–231. doi: 10.1016/0022-0981(91)90177-X

DIN EN ISO 11732-E23. (2005). *Water quality – Determination of ammonium nitrogen – Method by flow analysis (CFA and FIA) and spectrometric detection (E23)*. Beuth, Berlin.

DIN EN ISO 13395-D28. (1996). *Water quality – Determination of nitrite nitrogen and nitrate nitrogen and the sum of both by flow analysis (CFA and FIA) and spectrometric detection (D 28)*. Beuth, Berlin.

DIN EN ISO 15681 Part 2-D46. (2005). *Water quality – Determination of orthophosphate and total phosphorus contents by flow analysis (FIA and CFA) – Part 2: Method by continuous flow analysis (CFA) (D46)*. Beuth, Berlin.

Döll, P., and Schmied, H. M. (2012). How is the impact of climate change on river flow regimes related to the impact on mean annual runoff? A global-scale analysis. *Environ. Res. Lett.* 7:014037. doi: 10.1088/1748-9326/7/1/014037

Dopheide, A., Lear, G., He, Z., Zhou, J., and Lewis, G. D. (2015). Functional gene composition, diversity and redundancy in microbial stream biofilm communities. *PLoS One* 10:e0123179. doi: 10.1371/journal.pone.0123179

Dudgeon, D., Arthington, A. H., Gessner, M. O., Kawabata, Z. I., Knowler, D. J., Lévêque, C., et al. (2006). Freshwater biodiversity: importance, threats, status and conservation challenges. *Biol. Rev. Camb. Philos. Soc.* 81, 163–182. doi: 10.1017/S1464793105006950

DWD Climate Data Center (CDC). (2020). *Multi-annual station means for the climate normal reference period 1981-2010, for current station location and for reference station location Version V0.x*. Deutscher Wetterdienst, Offenbach.

Edgar, R. C. (2013). UPARSE: highly accurate OTU sequences from microbial amplicon reads. *Nat. Methods* 10, 996–998. doi: 10.1038/nmeth.2604

Edgar, R. C., and Flyvbjerg, H. (2015). Error filtering, pair assembly and error correction for next-generation sequencing reads. *Bioinformatics* 31, 3476–3482. doi: 10.1093/bioinformatics/btv401

Edgar, R. C., Haas, B. J., Clemente, J. C., Quince, C., and Knight, R. (2011). UCHIME improves sensitivity and speed of chimera detection. *Bioinformatics* 27, 2194–2200. doi: 10.1093/bioinformatics/btr381

Elosegi, A., Díez, J., and Mutz, M. (2010). Effects of hydromorphological integrity on biodiversity and functioning of river ecosystems. *Hydrobiologia* 657, 199–215. doi: 10.1007/s10750-009-0083-4

Evans, S. E., and Wallenstein, M. D. (2012). Soil microbial community response to drying and rewetting stress: does historical precipitation regime matter? *Biogeochemistry* 109, 101–116. doi: 10.1007/s10533-011-9638-3

Fazi, S., Vázquez, E., Casamayor, E. O., Amalfitano, S., and Butturini, A. (2013). Stream hydrological fragmentation drives bacterioplankton community composition. *PLoS One* 8:e64109. doi: 10.1371/journal.pone.0064109

Febria, C. M., Beddoes, P., Fulthorpe, R. R., and Williams, D. D. (2012). Bacterial community dynamics in the hyporheic zone of an intermittent stream. *ISME J.* 6, 1078–1088. doi: 10.1038/ismej.2011.173

Feio, M. J., Alves, T., Boavida, M., Medeiros, A., and Graça, M. A. S. (2010). Functional indicators of stream health: a river-basin approach. *Freshw. Biol.* 55, 1050–1065. doi: 10.1111/j.1365-2427.2009.02332.x

Fellows, C. S., Clapcott, J. E., Udy, J. W., Bunn, S. E., Harch, B. D., Smith, M. J., et al. (2006). Benthic metabolism as an indicator of stream ecosystem health. *Hydrobiologia* 572, 71–87. doi: 10.1007/s10750-005-9001-6

Feng, K., Zhang, Z., and Cai, W. (2017). Biodiversity and species competition regulate the resilience of microbial biofilm community. *Mol. Ecol.* 26, 6170–6182.

Folke, C., Carpenter, S., Walker, B., Scheffer, M., Elmqvist, T., Gunderson, L., et al. (2004). Regime shifts, resilience, and biodiversity in ecosystem management. *Annu. Rev. Ecol. Evol. Syst.* 35, 557–581. doi: 10.1146/annurev.ecolsys.35.021103.105711

Franzosa, E. A., Hsu, T., Sirota-Madi, A., Shafquat, A., Abu-Ali, G., Morgan, X. C., et al. (2015). Sequencing and beyond: integrating molecular "omics" for microbial community profiling. *Nat. Rev. Microbiol.* 13, 360–372. doi: 10.1038/nrmicro3451

Freimann, R., Bürgmann, H., Findlay, S. E. G., and Robinson, C. T. (2013). Bacterial structures and ecosystem functions in glaciated floodplains: contemporary states and potential future shifts. *ISME J.* 7, 2361–2373. doi: 10.1038/ismej.2013.114

Frey, B., Rime, T., Phillips, M., Stierli, B., Hajdas, I., Widmer, F., et al. (2016). Microbial diversity in European alpine permafrost and active layers. *FEMS Microbiol. Ecol.* 92:fiw018. doi: 10.1093/femsec/fiw018

Frossard, A., Gerull, L., Mutz, M., and Gessner, M. O. (2012). Disconnect of microbial structure and function: enzyme activities and bacterial communities in nascent stream corridors. *ISME J.* 6, 680–691. doi: 10.1038/ismej.2011.134

Gaarder, T., and Gran, H. H. (1927). Investigations of the production of phytoplankton in the Oslo Fjord. *Rapports et procès-verbaux des réunions/Conseil international pour l'exploration de la mer* 42, 1–48.

Galand, P. E., Pereira, O., and Hochart, C. A. (2018). Strong link between marine microbial community composition and function challenges the idea of functional redundancy. *ISME J.* 12, 2470–2478.

Gionchetta, G., Artigas, J., Arias-Real, R., Oliva, F., and Romaní, A. M. (2020). Multi-model assessment of hydrological and environmental impacts on streambed microbes in Mediterranean catchments. *Environ. Microbiol.* 22, 2213–2229. doi: 10.1111/1462-2920.14990

Gionchetta, G., Oliva, F., Menéndez, M., Lopez Laseras, P., and Romaní, A. M. (2019). Key role of streambed moisture and flash storms for microbial resistance and resilience to long-term drought. *Freshw. Biol.* 64, 306–322. doi: 10.1111/fwb.13218

Goldman, A. E., Graham, E. B., Crump, A. R., Kennedy, D. W., Romero, E. B., Anderson, C. G., et al. (2017). Biogeochemical cycling at the aquatic-terrestrial interface is linked to parafluvial hyporheic zone inundation history. *Biogeosciences* 14, 4229–4241. doi: 10.5194/bg-14-4229-2017

Gómez-Gener, L., Obrador, B., Marcé, R., Acuña, V., Catalán, N., Casas-Ruiz, J. P., et al. (2016). When water vanishes: magnitude and regulation of carbon dioxide emissions from dry temporary streams. *Ecosystems* 19, 710–723. doi: 10.1007/s10021-016-9963-4

Gossiaux, A., Jabiol, J., Poupin, P., Chauvet, E., and Guérold, F. (2019). Seasonal variations overwhelm temperature effects on microbial processes in headwater streams: insights from a temperate thermal spring. *Aquat. Sci.* 81, 1–11. doi: 10.1007/s00027-019-0627-2

Gostinčar, C., Muggia, L., and Grube, M. (2012). Polyextremotolerant black fungi: oligotrophism, adaptive potential, and a link to lichen symbioses. *Front. Microbiol.* 3, 1–6. doi: 10.3389/fmicb.2012.00390

Graeber, D., Jensen, T. M., Rasmussen, J. J., Riis, T., Wiberg-Larsen, P., and Baattrup-Pedersen, A. (2017). Multiple stress response of lowland stream benthic macroinvertebrates depends on habitat type. *Sci. Total Environ.* 599-600, 1517–1523. doi: 10.1016/j.scitotenv.2017.05.102

Han, M. S., and Furuya, K. (2000). Size and species-specific primary productivity and community structure of phytoplankton in Tokyo Bay. *J. Plankton Res.* 22, 1221–1235. doi: 10.1093/plankt/22.7.1221

Harvey, J. W., Drummond, J. D., Martin, R. L., McPhillips, L. E., Packman, A. I., Jerolmack, D. J., et al. (2012). Hydrogeomorphology of the hyporheic zone: stream solute and fine particle interactions with a dynamic streambed. *J. Geophys. Res. Biogeo.* 117, 1–20. doi: 10.1029/2012JG002043

Hawkes, C. V., and Keitt, T. H. (2015). Resilience vs. historical contingency in microbial responses to environmental change. *Ecol. Lett.* 18, 612–625.

Holling, C. S. (1973). Resilience and stability of ecological systems. *Annu. Rev. Ecol. Evol. Syst.* 4, 1–23. doi: 10.1146/annurev.es.04.110173.000245

Hullar, M. A. J., Kaplan, L. A., and Stahl, D. A. (2006). Recurring seasonal dynamics of microbial communities in stream habitats. *Appl. Environ. Microbiol.* 72, 713–722. doi: 10.1128/AEM.72.1.713-722.2006

Jansson, J. K., Neufeld, J. D., Moran, M. A., and Gilbert, J. A. (2012). Omics for understanding microbial functional dynamics. *Environ. Microbiol.* 14, 1–3. doi: 10.1111/j.1462-2920.2011.02518.x

Kearns, P. J., and Shade, A. (2018). Trait-based patterns of microbial dynamics in dormancy potential and heterotrophic strategy: case studies of resource-based and post-press succession. *ISME J.* 12, 2575–2581. doi: 10.1038/s41396-018-0194-x

Kõljalg, U., Nilsson, H. R., Schigel, D., Tedersoo, L., Larsson, K. H., May, T. W., et al. (2020). The taxon hypothesis paradigm – on the unambiguous detection and communication of taxa. *Microorganisms* 8, 1–24. doi: 10.3390/microorganisms8121910

König, S., Worrich, A., Centler, F., Wick, L. Y., Miltner, A., Kästner, M., et al. (2017). Modelling functional resilience of microbial ecosystems: analysis of governing processes. *Environ Model Softw.* 89, 31–39. doi: 10.1016/j.envsoft.2016.11.025

Langenheder, S., Lindström, E. S., and Tranvik, L. J. (2005). Weak coupling between community composition and functioning of aquatic bacteria. *Limnol. Oceanogr.* 50, 957–967. doi: 10.4319/lo.2005.50.3.0957

Langlois, V., and Valance, A. (2007). Initiation and evolution of current ripples on a flat sand bed under turbulent water flow. *Eur Phys J E* 22, 201–208. doi: 10.1140/epje/e2007-00023-0

Larned, S. T., Datry, T., Arscott, D. B., and Tockner, K. (2010). Emerging concepts in temporary-river ecology. *Freshw. Biol.* 55, 717–738. doi: 10.1111/j.1365-2427.2009.02322.x

Lau, K. E. M., Washington, V. J., Fan, V., Neale, M. W., Lear, G., Curran, J., et al. (2015). A novel bacterial community index to assess stream ecological health. *Freshw. Biol.* 60, 1988–2002. doi: 10.1111/fwb.12625

Lawton, J. H., and Brown, V. K. (1993). "Redundancy in ecosystems" in *Biodiversity and ecosystem function.* eds. E.-D. Schulze and H. A. Mooney (Heidelberg: Springer), 255–270.

Lecerf, A. (2017). Methods for estimating the effect of litterbag mesh size on decomposition. *Ecol. Model.* 362, 65–68. doi: 10.1016/j.ecolmodel.2017.08.011

Ledger, M. E., Brown, L. E., Edwards, F. K., Hudson, L. N., Milner, A. M., and Woodward, G. (2013). Extreme climatic events alter aquatic food webs: a synthesis of evidence from a mesocosm drought experiment. *Adv. Ecol. Res.* 48, 343–395. doi: 10.1016/B978-0-12-417199-2.00006-9

Leff, L., Van Gray, J. B., Martí, E., Merbt, S. N., and Romaní, A. M. (2016). "Aquatic biofilms and biogeochemical processes" in *Aquatic biofilms: Ecology, water quality and wastewater treatment.* eds. A. M. Romaní, H. Guasch and M. Dolors Balaguer (Poole: Caister Academic Press), 89–108.

Lenth, R. (2023). *_emmeans: Estimated Marginal Means, aka Least-Squares Means_. R package version 1.8.4-1.* Available at: https://CRAN.R-project.org/package=emmeans.

Loreau, M. (2004). Does functional redundancy exist? *Oikos* 104, 606–611. doi: 10.1111/j.0030-1299.2004.12685.x

Louca, S., Polz, M. F., Mazel, F., Albright, M. B. N., Huber, J. A., O'Connor, M. I., et al. (2018). Function and functional redundancy in microbial systems. *Nat Ecol Evolut* 2, 936–943. doi: 10.1038/s41559-018-0519-1

Mapelli, V., Olsson, L., and Nielsen, J. (2008). Metabolic footprinting in microbiology: methods and applications in functional genomics and biotechnology. *Trends Biotechnol.* 26, 490–497. doi: 10.1016/j.tibtech.2008.05.008

Marcarelli, A. M., Huckins, C. J., and Eggert, S. L. (2015). Sand aggradation alters biofilm standing crop and metabolism in a low-gradient Lake Superior tributary. *J. Great Lakes Res.* 41, 1052–1059. doi: 10.1016/j.jglr.2015.09.004

Martin, M. (2011). Cutadapt removes adapter sequences from high-throughput sequencing reads. *EMBnet J.* 17, 10–12. doi: 10.14806/ej.17.1.200

Marxsen, J., Zoppini, A., and Wilczek, S. (2010). Microbial communities in streambed sediments recovering from desiccation. *FEMS Microbiol. Ecol.* 71, 374–386. doi: 10.1111/j.1574-6941.2009.00819.x

Mathooko, J. M., Mpawenayo, B., Kipkemboi, J. K., and M'erimba, C. M. (2005). Distributional patterns of diatoms and Limnodrilus oligochaetes in a Kenyan dry streambed following the 1999-2000 drought conditions. *Int. Rev. Hydrobiol.* 90, 185–200. doi: 10.1002/iroh.200310708

Matthaei, C. D., Weller, F., Kelly, D. W., and Townsend, C. R. (2006). Impacts of fine sediment addition to tussock, pasture, dairy and deer farming streams in New Zealand. *Freshw. Biol.* 51, 2154–2172. doi: 10.1111/j.1365-2427.2006.01643.x

McCormick, A. R., Phillips, J. S., and Ives, A. R. (2019). Responses of benthic algae to nutrient enrichment in a shallow lake: linking community production, biomass, and composition. *Freshw. Biol.* 64, 1833–1847. doi: 10.1111/fwb.13375

McKew, B. A., Taylor, J. D., McGenity, T. J., and Underwood, G. J. C. (2011). Resistance and resilience of benthic biofilm communities from a temperate saltmarsh to desiccation and rewetting. *ISME J.* 5, 30–41. doi: 10.1038/ismej.2010.91

Mendoza-Lera, C., Frossard, A., Knie, M., Federlein, L. L., Gessner, M. O., and Mutz, M. (2017). Importance of advective mass transfer and sediment surface area for streambed microbial communities. *Freshw. Biol.* 62, 133–145. doi: 10.1111/fwb.12856

Meyer, J. L., Strayer, D. L., Wallace, J. B., Eggert, S. L., Helfman, G. S., and Leonard, N. E. (2007). The contribution of headwater streams to biodiversity in river networks. *J. Am. Water Resour. Assoc.* 43, 86–103. doi: 10.1111/j.1752-1688.2007.00008.x

Miller, A. R., Lowe, R. L., and Rotenberry, J. T. (1987). Succession of diatom communities on sand grains. *J. Ecol.* 75, 693–709. doi: 10.2307/2260200

Muñoz, I., Abril, M., Casas-Ruiz, J. P., Casellas, M., Gómez-Gener, L., Marcé, R., et al. (2018). Does the severity of non-flow periods influence ecosystem structure and function of temporary streams? A mesocosm study. *Freshw. Biol.* 63, 613–625. doi: 10.1111/fwb.13098

Naiman, R. J., Decamps, H., and Pollock, M. (1993). The role of riparian corridors in maintaining regional biodiversity. *Ecol. Appl.* 3, 209–212. doi: 10.2307/1941822

Niemi, G. J., DeVore, P., Detenbeck, N., Taylor, D., Lima, A., Pastor, J., et al. (1990). Overview of case studies on recovery of aquatic systems from disturbance. *Environ. Manag.* 14, 571–587. doi: 10.1007/BF02394710

Nikolenko, S. I., Korobeynikov, A., and Alekseyev, M. (2013). BAYESHAMMER: Bayesian subclustering for error correction in single cell sequencing. *BMC Genomics* 14:S7. doi: 10.1186/1471-2164-14-S1-S7

Nõges, P., Argillier, C., Borja, Á., Garmendia, J. M., Hanganu, J., Kodeš, V., et al. (2016). Quantified biotic and abiotic responses to multiple stress in freshwater, marine and ground waters. *Sci. Total Environ.* 540, 43–52. doi: 10.1016/j.scitotenv.2015.06.045

Oksanen, J., Simpson, G., Blanchet, F., Kindt, R., Legendre, P., Minchin, P., et al. (2022). _vegan: Community Ecology Package_. R package version 2.6-4. Available at: https://CRAN.R-project.org/package=vegan

Oprei, A., Zlatanović, S., and Mutz, M. (2019). Grazers superimpose humidity effect on stream biofilm resistance and resilience to dry-rewet stress. *Sci. Total Environ.* 659, 841–850. doi: 10.1016/j.scitotenv.2018.12.316

Packman, A. I., and Brooks, N. H. (2001). Hyporheic exchange of solutes and colloids with moving bed forms. *Water Resour. Res.* 37, 2591–2605. doi: 10.1029/2001WR000477

Paruch, L., Paruch, A. M., Eiken, H. G., Skogen, M., and Sørheim, R. (2020). Seasonal dynamics of lotic bacterial communities assessed by 16S rRNA gene amplicon deep sequencing. *Sci. Rep.* 10, 16399–16310. doi: 10.1038/s41598-020-73293-9

Pelletier, M. C., Ebersole, J., Mulvaney, K., Rashleigh, B., Gutierrez, M. N., Chintala, M., et al. (2020). Resilience of aquatic systems: review and management implications. *Aquat. Sci.* 82, 1–44. doi: 10.1007/s00027-020-00717-z

Perez-Mon, C., Frey, B., and Frossard, A. (2020). Functional and structural responses of arctic and alpine soil prokaryotic and fungal communities under freeze-thaw cycles of different frequencies. *Front. Microbiol.* 11:982. doi: 10.3389/fmicb.2020.00982

Peter, H., Ylla, I., and Gudasz, C. (2011). Multifunctionality and Diversity in Bacterial Biofilms. *PLoS One* 6:e23225.

Piano, E., Falasco, E., and Bona, F. (2017). Mediterranean rivers: consequences of water scarcity on benthic algal chlorophyll a content. *J. Limnol.* 76, 39–48. doi: 10.4081/jlimnol.2016.1503

Pimm, S. L. (1984). The complexity and stability of ecosystems. *Nature* 307, 321–326. doi: 10.1038/307321a0

Pohlon, E., Fandino, A. O., and Marxsen, J. (2013). Bacterial community composition and extracellular enzyme activity in temperate streambed sediment during drying and rewetting. *PLoS One* 8:e83365. doi: 10.1371/journal.pone.0083365

Power, M. (1998). Recovery in aquatic ecosystems: an overview of knowledge and needs. *J. Aquat. Ecosyst. Stress. Recover.* 6, 253–257. doi: 10.1023/A:1009991620319

Quast, C., Pruesse, E., Yilmaz, P., Gerken, J., Schweer, T., Yarza, P., et al. (2013). The SILVA ribosomal RNA gene database project: improved data processing and web-based tools. *Nucleic Acids Res.* 41, D590–D596. doi: 10.1093/nar/gks1219

R Core Team. (2021). *R: A language and environment for statistical computing*. R Foundation for Statistical Computing, Vienna, Austria.

Raymond, P. A., Hartmann, J., Lauerwald, R., Sobek, S., McDonald, C., Hoover, M., et al. (2013). Global carbon dioxide emissions from inland waters. *Nature* 503, 355–359. doi: 10.1038/nature12760

Rees, G. N., Watson, G. O., Baldwin, D. S., and Mitchell, A. M. (2006). Variability in sediment microbial communities in a semipermanent stream: impact of drought. *J. N. Am. Benthol. Soc.* 25, 370–378. doi: 10.1899/0887-3593(2006)25[370:VISMCI]2.0.CO;2

Rocca, J. D., Simonin, M., Blaszczak, J. R., Ernakovich, J. G., Gibbons, S. M., Midani, F. S., et al. (2019). The microbiome stress project: toward a global meta-analysis of environmental stressors and their effects on microbial communities. *Front. Microbiol.* 9, 1–14. doi: 10.3389/fmicb.2018.03272

Romaní, A. M., Amalfitano, S., Artigas, J., Fazi, S., Sabater, S., Timoner, X., et al. (2013). Microbial biofilm structure and organic matter use in Mediterranean streams. *Hydrobiologia* 719, 43–58. doi: 10.1007/s10750-012-1302-y

Romaní, A. M., Chauvet, E., Febria, C., Mora-Gómez, J., Risse-Buhl, U., Timoner, X., et al. (2017). "The biota of intermittent rivers and ephemeral streams: prokaryotes, fungi, and protozoans" in *Intermittent Rivers and ephemeral streams*. eds. T. Datry, N. Bonada and A. Boulton (Burlington: Academic Press), 161–188.

Romaní, A. M., and Sabater, S. (2000). Influence of algal biomass on extracellular enzyme activity in river biofilms. *Microb. Ecol.* 40, 16–24. doi: 10.1007/s002480000041

Romero, F., Sabater, S., Timoner, X., and Acuña, V. (2018). Multistressor effects on river biofilms under global change conditions. *Sci. Total Environ.* 627, 1–10. doi: 10.1016/j.scitotenv.2018.01.161

Rutherford, J. C., Latimer, G. J., and Smith, R. K. (1993). Bedform mobility and benthic oxygen uptake. *Water Res.* 27, 1545–1558. doi: 10.1016/0043-1354(93)90099-4

Sabater, S., Timoner, X., Borrego, C., and Acuña, V. (2016). Stream biofilm responses to flow intermittency: from cells to ecosystems. *Front. Environ. Sci.* 4, 1–10. doi: 10.3389/fenvs.2016.00014

Santschi, F., Gounand, I., and Harvey, E. (2018). Leaf litter diversity and structure of microbial decomposer communities modulate litter decomposition in aquatic systems. *Funct. Ecol.* 32, 522–532.

Scheidweiler, D., Mendoza-Lera, C., Mutz, M., and Risse-Buhl, U. (2021). Overlooked implication of sediment transport at low flow: migrating ripples modulate streambed phototrophic and heterotrophic microbial activity. *Water Resour. Res.* 57, 1–16. doi: 10.1029/2020WR027988

Schloss, P. D., Westcott, S. L., Ryabin, T., Hall, J. R., Hartmann, M., Hollister, E. B., et al. (2009). Introducing mothur: open-source, platform-independent, community-supported software for describing and comparing microbial communities. *Appl. Environ. Microbiol.* 75, 7537–7541. doi: 10.1128/AEM.01541-09

Schreckinger, J., Mutz, M., Mendoza-Lera, C., and Frossard, A. (2021). Attributes of drying define the structure and functioning of microbial communities in temperate riverbed sediment. *Front. Microbiol.* 12, 1–15. doi: 10.3389/fmicb.2021.676615

Shade, A., Peter, H., Allison, S. D., Baho, D. L., Berga, M., Bürgmann, H., et al. (2012). Fundamentals of microbial community resistance and resilience. *Front. Microbiol.* 3, 1–19. doi: 10.3389/fmicb.2012.00417

Smeti, E., von Schiller, D., Karaouzas, I., Laschou, S., Vardakas, L., Sabater, S., et al. (2019). Multiple stressor effects on biodiversity and ecosystem functioning in a Mediterranean temporary river. *Sci. Total Environ.* 647, 1179–1187. doi: 10.1016/j.scitotenv.2018.08.105

Song, H. S., Cannon, W. R., and Beliaev, A. S. (2014). Mathematical modeling of microbial community dynamics: A methodological review. *Processes* 2, 711–752.

Sorensen, J. W., and Shade, A. (2020). Dormancy dynamics and dispersal contribute to soil microbiome resilience. *Philosoph. Transac R Soc B Biol Sci* 375:20190255. doi: 10.1098/rstb.2019.0255

Streble, H., and Krauter, D. (1988). *Das Leben im Wassertropfen: Mikroflora und Mikrofauna des Süsswassers; ein Bestimmungsbuch; neu: biologische Gewässeranalyse*. Stuttgart: Franckh-Kosmos.

Steudel, B., Hector, A., and Friedl, T. (2012). Biodiversity effects on ecosystem functioning change along environmental stress gradients. *Ecol. Lett.* 15, 1397–1405.

Timoner, X., Acuña, V., Von Schiller, D., and Sabater, S. (2012). Functional responses of stream biofilms to flow cessation, desiccation and rewetting. *Freshw. Biol.* 57, 1565–1578. doi: 10.1111/j.1365-2427.2012.02818.x

Timoner, X., Colls, M., Salomón, S. M., Oliva, F., Acuña, V., and Sabater, S. (2020). Does biofilm origin matter? Biofilm responses to non-flow period in permanent and temporary streams. *Freshw. Biol.* 65, 514–523. doi: 10.1111/fwb.13447

Truchy, A., Sarremejane, R., Muotka, T., Mykrä, H., Angeler, D. G., Lehosmaa, K., et al. (2020). Habitat patchiness, ecological connectivity and the uneven recovery of boreal stream ecosystems from an experimental drought. *Glob. Chang. Biol.* 26, 3455–3472. doi: 10.1111/gcb.15063

Uehlinger, U., Naegeli, M., and Fisher, S. G. (2002). A heterotrophic desert stream? The role of sediment stability. *Western North Am Nat* 62, 466–473.

van Den Brink, P. J., and Ter Braak, C. J. F. (1999). Principal response curves: analysis of time-dependent multivariate responses of biological community to stress. *Environ. Toxicol. Chem.* 18, 138–148. doi: 10.1002/etc.5620180207

van Kruistum, H., Bodelier, P. L. E., Ho, A., Meima-Franke, M., and Veraart, A. J. (2018). Resistance and recovery of methane-oxidizing communities depends on stress regime and history; a microcosm study. *Front. Microbiol.* 9:1714. doi: 10.3389/fmicb.2018.01714

Vass, M., and Langenheder, S. (2017). The legacy of the past: effects of historical processes on microbial metacommunities. *Aquat. Microb. Ecol.* 79, 13–19. doi: 10.3354/ame01816

Vázquez, E., Ejarque, E., Ylla, I., Romaní, A. M., and Butturini, A. (2015). Impact of drying/rewetting cycles on the bioavailability of dissolved organic matter molecular-weight fractions in a Mediterranean stream. *Freshwater Sci* 34, 263–275. doi: 10.1086/679616

Veach, A. M., Stegen, J. C., Brown, S. P., Dodds, W. K., and Jumpponen, A. (2016). Spatial and successional dynamics of microbial biofilm communities in a grassland stream ecosystem. *Mol. Ecol.* 25, 4674–4688. doi: 10.1111/mec.13784

von Berg, K.-H. L., Hoef-Emden, K., Birger, M., and Melkonian, M. (2012). *Der Kosmos-Algenführer: Süßwasseralgen unter dem Mikroskop: ein bestimmungsbuch*. Stuttgart: Kosmos.

von Schiller, D., Bernal, S., Dahm, C. N., and Martí, E. (2017). "Nutrient and organic matter dynamics in intermittent rivers and ephemeral streams" in *Intermittent rivers and ephemeral streams. Ecology and management*. eds. T. Datry, N. Bonada and A. Boulton (Burlington: Academic Press), 135–160.

Vörösmarty, C. J., Green, P., Salisbury, J., and Lammers, R. B. (2000). Global water resources: vulnerability from climate change and population growth. *Science* 289, 284–288. doi: 10.1126/science.289.5477.284

Wanders, N., and Van Lanen, H. A. J. (2015). Future discharge drought across climate regions around the world modelled with a synthetic hydrological modelling approach forced by three general circulation models. *Nat. Hazards Earth Syst. Sci.* 15, 487–504. doi: 10.5194/nhess-15-487-2015

Wheeler, B., and Torchiano, M. (2016). *lmPerm: permutation tests for linear models. R Package Version 2.1.0*. Available at: https://CRAN.R-project.org/package=lmPerm

Wieder, W. R., Allison, S. D., and Davidson, E. A. (2015). Explicitly representing soil microbial processes in Earth system models. *Global Biogeochem. Cycles* 29, 1782–1800.

Wilczek, S., Fischer, H., and Pusch, M. T. (2005). Regulation and seasonal dynamics of extracellular enzyme activities in the sediments of a large lowland river. *Microb. Ecol.* 50, 253–267. doi: 10.1007/s00248-004-0119-2

Wilkes, M. A., Gittins, J. R., Mathers, K. L., Mason, R., Casas-Mulet, R., Vanzo, D., et al. (2019). Physical and biological controls on fine sediment transport and storage in rivers. *Wiley Interdiscip. Rev. Water* 6:e1331. doi: 10.1002/wat2.1331

Winkler, J. P., Cherry, R. S., and Schlesinger, W. H. (1996). The Q10 relationship of microbial respiration in a temperate forest soil. *Soil Biol. Biochem.* 28, 1067–1072. doi: 10.1016/0038-0717(96)00076-4

Wohl, D. L., Arora, S., and Gladstone, J. R. (2004). Functional redundancy supports biodiversity and ecosystem function in a closed and constant environment. *Ecology* 85, 1534–1540. doi: 10.1890/03-3050

Wolke, P., Teitelbaum, Y., Deng, C., Lewandowski, J., and Arnon, S. (2020). Impact of bed form celerity on oxygen dynamics in the hyporheic zone. *Water* 12, 5–7. doi: 10.3390/w12010062

Woodward, G., Bonada, N., Feeley, H. B., and Giller, P. S. (2015). Resilience of a stream community to extreme climatic events and long-term recovery from a catastrophic flood. *Freshw. Biol.* 60, 2497–2510. doi: 10.1111/fwb.12592

Xiao, H. S., Chen, R. Y., Cheng, T. L., Fang, W. T., Hsu, C. H., and Chou, J. Y. (2019). Phenotypic plasticity in Aureobasidium pullulans isolates. *Int. J. Agric. Biol.* 22, 167–177. doi: 10.17957/IJAB/15.1047

Ylla, I., Sanpera-Calbet, I., Vázquez, E., Romaní, A. M., Muñoz, I., Butturini, A., et al. (2010). Organic matter availability during pre- and post-drought periods in a Mediterranean stream. *Hydrobiologia* 657, 217–232. doi: 10.1007/s10750-010-0193-z

Young, R. G., and Collier, K. J. (2009). Contrasting responses to catchment modification among a range of functional and structural indicators of river ecosystem health. *Freshw. Biol.* 54, 2155–2170. doi: 10.1111/j.1365-2427.2009.02239.x

Young, R. G., Matthaei, C. D., and Townsend, C. R. (2008). Organic matter breakdown and ecosystem metabolism: functional indicators for assessing river ecosystem health. *J. N. Am. Benthol. Soc.* 27, 605–625. doi: 10.1899/07-121.1

Zhai, J., Cong, L., Yan, G., Wu, Y., Liu, J., Wang, Y., et al. (2019). Influence of fungi and bag mesh size on litter decomposition and water quality. *Environ. Sci. Pollut. Res.* 26, 18304–18315. doi: 10.1007/s11356-019-04988-4

Zheng, L., Cardenas, M. B., Wang, L., and Mohrig, D. (2019). Ripple effects: bed form morphodynamics cascading into hyporheic zone biogeochemistry. *Water Resour. Res.* 55, 7320–7342. doi: 10.1029/2018WR023517

Zlatanović, S., Fabian, J., Mendoza-Lera, C., Woodward, K. B., Premke, K., and Mutz, M. (2017). Periodic sediment shift in migrating ripples influences benthic microbial activity. *Water Resour. Res.* 53, 4741–4755. doi: 10.1002/2017WR020656